Sources and distribution of organic matter in northern Patagonia fjords, Chile (~44–47° S): a multi–tracer approach for carbon cycling assessment

Julio Sepúlveda[a,*], Silvio Pantoja[b], Konrad A. Hughen[c]

[a] Department of Earth, Atmospheric and Planetary Sciences, Massachusetts Institute of Technology, 45 Carleton Street, E25–623, Cambridge MA 02139, USA

[b] Department of Oceanography and Center for Oceanographic Research in the eastern South Pacific, and COPAS Sur–Austral, University of Concepción, Casilla 160–C, Concepción, Chile

[c] Department of Marine Chemistry and Geochemistry, Woods Hole Oceanographic Institution, MS#25, Woods Hole, MA 02543, USA

*Corresponding author: Telephone: (1–617) 324–3954; Fax: (1–617) 253–8630; Email: juliosep@mit.edu (J. Sepúlveda)

Abstract

We investigated the provenance of organic matter in the inner fjord area of northern Patagonia, Chile (~44–47° S), by studying the elemental (organic carbon, total nitrogen), isotopic ($\delta^{13}C$, $\delta^{15}N$), and biomarker (*n*–alkanoic acids from vascular plant waxes) composition of surface sediments as well as local marine and terrestrial organic matter. Average end–member values of N/C, $\delta^{13}C$, and $\delta^{15}N$ from organic matter were 0.127 ± 0.010, –19.8 ± 0.3‰, and 9.9 ± 0.5‰ for autochthonous (marine) sources and 0.040 ± 0.018, –29.3 ± 2.1‰, 0.2 ± 3.0‰ for allochthonous (terrestrial) sources. Using a mixing equation based on these two end–members, we calculated the relative contribution of marine and terrestrial organic carbon from the open ocean to the heads of fjords close to river outlets. The input of marine–derived organic carbon varied widely and accounted for 13 to 96% (average 61%) of the organic carbon pool of surface sediments. Integrated regional calculations for the inner fjord system of northern Patagonia, which encompasses an area of ~ 4,280 km^2, suggest that carbon accumulation may account for between 2.3 and 7.8 x 10^4 ton C yr^{-1}. This represents a storage capacity of marine–derived carbon between 1.8 and 6.2 x 10^4 tons yr^{-1}, which corresponds to an assimilation rate of CO_2 by marine photosynthesis between 0.06 and 0.23 x 10^6 tons yr^{-1}. This rate suggests that the entire fjord system of Patagonia, which covers an area of ~ 240,000 km^2, may represent a potentially important region for the global burial of marine organic matter and the sequestration of atmospheric CO_2.

Keywords: organic matter sources; carbon cycling; CO_2; fjords; northern Patagonia; Chile

1. Introduction

Continental margins are important components of the global carbon cycle and may be responsible for >40% of the carbon sequestration in the ocean (Hedges and Keil, 1995; Muller–Karger et al., 2005). This property is due to high rates of primary production and burial of organic matter in sediments, mainly where rivers supply large amounts of fine sediments (de Haas et al., 2002, and references therein). High–latitude fjords such as those located in the Northern Hemisphere have been shown to be important sites for carbon burial (e.g., St–Onge and Hillaire–Marcel, 2001) and CO_2 sequestration (Winkelmann and Knies, 2005). Due to their proximity to the continent and semi–restricted location, the organic matter deposited in the fjord sediments comprises mixtures of marine (autochthonous), terrestrial (allochthonous), and anthropogenic sources with different levels of reactivity (e.g., Meyers, 1994). Therefore, in order to assess the cycling of organic carbon in fjord systems, a geochemical characterization of its multiple potential sources is essential.

The elemental (C/N) and stable isotope ($\delta^{13}C$, $\delta^{15}N$) composition of organic matter can be used for tracing multiple sources of organic matter in coastal sedimentary environments (e.g., Goñi et al., 2003; Maksymowska et al., 2000; Meyers, 1994, 1997; Müller, 2001; Perdue and Koprivnjak, 2007; Thornton and McManus, 1994; Winkelmann and Knies, 2005). This is due to the distinguishable elemental and isotopic composition of marine and terrestrial organic matter. Typical C/N ratios in marine organic matter range between 4 and 10 whereas in vascular land plants, these ratios are over 20 (e.g., Meyers, 1994, 1997). Organic matter produced by marine organisms exhibits $\delta^{13}C$ values between –20 and –22‰ (e.g., Meyers, 1994), but organic matter produced by land plants using the C_3 pathway, typical of high–latitude regions like the Chilean Patagonia, averages –27‰ (O'Leary,

1981). The $\delta^{15}N$ of marine organic matter produced by phytoplankton ranges between 3 and 8‰ whereas the average $\delta^{15}N$ of terrestrial organic matter is 0.4‰ (Peters et al., 1978). Typical $\delta^{13}C$ values of organic matter carried by rivers vary between –35 and –25‰, but $\delta^{15}N$ values are about 5‰ (e.g., Meyers, 1997). Since the elemental and isotopic signatures of organic matter can be altered during early diagenesis (e.g., Freudenthal et al., 2001), the use of a multi–proxy approach is necessary to minimize potential biases in the interpretation of multiple sources from a single analysis. Recently, this approach has been applied to reconstruct changes in terrestrial input into the northern Patagonia fjord system over the last two millennia (Sepúlveda et al., 2009).

Additionally, molecular biomarkers can be related to more specific sources of organic matter. Long–chain *n*–alkyl lipids (consisting of *n*–alkanes, *n*–alkanols, and *n*–alkanoic acids) can be used to trace the input of terrestrial organic matter since they are found in the remains of vascular plants deposited in marine and lacustrine sediments (e.g., Huang et al., 1999, 2000; Ohkouchi et al., 1997). Long–chain *n*–alkyl lipids are major components of the epicuticular waxes of vascular plant leaves and contribute to preserving the water balance of the plant (Eglinton and Hamilton, 1967). Leaf waxes are relatively resistant to degradation (Cranwell, 1981) and are generally well preserved in the sedimentary record (Haddad et al., 1992; Logan et al., 1995). In plants, *n*–alkanoic acids occur as the *n*–C_{16}–C_{36} homologues and show a strong even–over–odd predominance, although the most common homologues are the *n*–C_{22}–C_{30} components (Eglinton and Hamilton, 1967). Additionally, the distribution of these homologues, parameterized as the average chain length index (ACL), has been used to distinguish vegetation from contrasting environmental conditions (e.g., Hughen et al., 2004; Sachse et al., 2006).

The coastline of Chile's northern Patagonian fjords (~44–47° S) is generally rugged, and the mainland coast is separated from the Pacific Ocean by a large number of islands and narrow channels. This estuarine system resulted from the erosive action of glaciers and the tectonic sinking of a longitudinal valley south of Puerto Montt (41°31'S) during the Quaternary (Borgel, 1970). The bottom topography of the main inlets is irregular, with depths ranging from <100 to 1,050 m (Araya, 1997; Pickard, 1971). The mean annual precipitation in the study area is ~3,000 mm $year^{-1}$ and the mean annual air temperature is ~10 °C (DGA, 2003). The most important rivers in the area are the Baker (1500 m^3 s^{-1}), Aysén (515 m^3 s^{-1}), Pascua (400 m^3 s^{-1}), Cisnes (190 m^3 s^{-1}), and Bravo (150 m^3 s^{-1}) rivers (DGA, 2003), whereas maximum outflows from the fjord system are observed at 42°, 46°, and 50° S (Dávila et al., 2002). The significant input of freshwater from river discharge and continental runoff results in an estuarine system with a stratified water column (Silva et al., 1995). Dense vegetation characteristic of cold, wet climate regimes surrounds the inner fjord area in the form of a temperate evergreen rain forest (e.g., Villagrán, 1988). The irregular bottom topography and the presence of shallow sills (DaSilva et al., 1997; Delgado, 2004) diminishes bottom water circulation (Pickard and Stanton, 1980; Silva et al., 1995), favoring high sedimentation rates (0.14–0.75 cm yr^{-1}; Rojas and Silva, 2005; Salamanca and Jara, 2003; Sepúlveda et al., 2005) and the preservation of organic matter (Rojas and Silva, 2005; Sepúlveda et al., 2005). Surface sediments of inner fjords between 44° and 46° S are of fine, mostly silt–clay material, although some areas are dominated by fine sand (Silva et al., 1998a). Total organic carbon and organic nitrogen vary between 0.1 and 3%, and between 0.01 and 0.4%, respectively (Silva et al., 1998a). The Chilean fjord system receives organic matter input in the form of marine primary production and land–

plant remains carried from the surrounding native forests by rivers and overland runoff. In addition, some shallow and semi–restricted areas evidence the anthropogenic impact of salmon farming activities (Soto and Norambuena, 2004). Estimates of primary production for the area between 44º and 46º S have resulted in values ranging between 0.01 and 0.82 g C m^{-2} d^{-1} in winter, 0.23 and 5.16 g C m^{-2} d^{-1} in spring, and 1.42 and 4.38 g C m^{-2} d^{-1} in summer (Aracena et al., this issue; Gonzalez et al., this issue; Pizarro et al., 2005;). A decrease in primary production is observed from the mouth of Moraleda Channel in the north to the Elefantes Gulf in the south, whereas the vertical flux of organic carbon at 50 meters is nearly twice as high in spring than in winter (González et al., this issue). Although several studies have previously characterized the bulk geochemistry of surface sediments in the Patagonian fjord system (e.g, Rojas and Silva, 2005; Silva et al., 1998a; Silva and Prego, 2002), studies characterizing the sources of organic matter into the system using local end–members are scarce (Silva et al., this issue; Vargas et al., this issue), and no previous research has focused on regional calculations of carbon cycling and carbon sequestration in this region.

In order to characterize the sources of organic matter in the fjord system of northern Patagonia, we studied the elemental and isotopic composition of carbon and nitrogen in surface sediments along a gradient from the open ocean to the inner fjords, including the characterization of local autochthonous (marine) and allochthonous (terrestrial; including riverine sediments and living and degraded land vegetation) end–members. Additionally, we used the concentration of *n*–alkanoic fatty acid leaf waxes as a supplementary indicator of terrestrial organic matter input. We present regional carbon mass accumulation rate calculations for the northern Patagonia fjord system and discuss the global importance of this area for the burial of marine organic matter and the sequestration of atmospheric CO_2.

2. Methods

2.1. Sampling

Sediment samples were obtained during the CIMAR–FIORDO 7 expedition (November 2001) aboard the R/V AGOR Vidal Gormaz of the Chilean Navy, using a box–corer at 14 stations in the inner fjord area between ~43°44'S and ~46º29'S in southern Chile (Fig. 1; Table 1). The sampling stations were located along a gradient of marine and freshwater influences in order to cover the entire range of organic matter sources feeding into the system, from the break in the continental shelf to the head of the inner fjords, including *Boca del Guafo*, Jacaf Fjord, Puyuhuapi Fjord, Ventisquero Sound, Quitralco Fjord, Cupquelan Fjord, and Elefantes Channel. Surface sediments from 0 to 1 cm were subsampled onboard using PVC tubes (7–cm diameter), stored in plastic bags, and frozen at –20 ºC until laboratory analyses. Additional samples were collected, including surface sediments from five rivers, fresh land vegetation (the most common and abundant species), and degraded vegetation (woody debris of leaves and wood fragments) from riverine sediments sieved through a 350–µm mesh (Fig. 1; Table 1). Subsurface (~5 m) water samples were taken from the ship inlet and ~5 L were filtered through a precombusted (450 °C, 4 h), 47–mm diameter, GF/F filter (0.7–µm pore size) to collect particulate organic matter. These samples were also stored at –20 °C until laboratory analyses.

2.2. Organic carbon, total nitrogen, and stable isotope analyses

Marine and riverine sediment samples were freeze–dried and then ground and homogenized in an agate mortar before processing. About 50 mg of sediment were weighed in tin cups and the carbonate was removed by acidifying with 50% v/v sulfurous acid.

Freeze–dried degraded and fresh vegetation samples were ground in an agate mortar and weighed in tin cups. River sediment samples were sieved through a 125–µm mesh to measure organic carbon associated with very fine sand, silt, and clay fractions (high mineral surface area according to Mayer, 1994a, b). Filters containing particulate matter were dried over–night at 60 °C and packaged in tin cups.

Organic carbon (C_{org}), total nitrogen, and bulk $\delta^{13}C$ and $\delta^{15}N$ were analyzed by elemental analysis and Isotope Ratio Mass Spectrometry at the University of California Davis Stable Isotope Facility. The precision of the $\delta^{13}C$ and $\delta^{15}N$ determinations was ± 0.03‰ and ± 0.08‰, respectively. Additional elemental and isotopic data from surface sediments of the continental slope off Chile between 41° S and 43°13'S were obtained from Hebbeln et al. (2000) (Table 1) and used for constraining the end–member values of marine–derived organic matter. C_{org}, $\delta^{13}C$, and porosity data from surface sediments in the inner fjord area (Moraleda, Costa, and Elefantes channels; Jacaf, Puyuhuapi, Aysén, Quitralco, and Cupquelan fjords) were obtained from previous expeditions in the study area (Pinto and Bonert, 2005; Rojas, 2002; Silva et al., 1998b, this issue) and used for constraining regional calculations of organic carbon burial.

2.3. Analysis of n–alkanoic fatty acid (FA) leaf waxes

Total lipids were extracted from freeze–dried marine and riverine sediments and plant leaves in an Accelerated Solvent Extraction System (DIONEX ASE 200) using a solvent mixture of CH_2Cl_2:MeOH 9:1 at 100 ºC and 1000 psi. The non–polar and polar fractions were separated in a LC–NH_2 column after eluting with 7 mL CH_2Cl_2:acetone (9:1) and 8 mL 2% formic acid in CH_2Cl_2, respectively. The polar fraction was transesterified with 0.5

mL BF3:MeOH at 70 °C for 20 min to convert free and esterified fatty acids into fatty acid methyl esters (FAMEs). Milli–Q water (20 mL) and hexane (10 mL) were added. The hexane fraction was subsequently removed, concentrated, and loaded onto a silica gel column (100–200 mesh, 5% water). FAMEs were eluted in the second fraction with 5% ethyl acetate in hexane. This fraction was transferred to a glass vial with inserts and re–dissolved in 50 μL toluene before injection onto a gas chromatograph.

Gas chromatography was carried out with a 60–m Chrompack capillary column (0.25–mm ID, 0.25–μm film thickness) using an Agilent 6850 GC coupled with an Agilent 6850 autosampler and a flame ionization detector. Hydrogen was used as a carrier gas and the column oven temperature was programmed from 60 ºC (1 min) to 210 ºC (8 min), to 330 ºC (53 min). $C_{16–32}$ *n*–alkanoic fatty acids were identified by their retention times and quantified by comparison with a mixture of nine authenticated reference standards.

3. Results and discussion

3.1. Elemental composition

The linear regression between total nitrogen and C_{org} (r^2 = 0.87) in surface sediments showed an intercept of –0.0064% total nitrogen (close to zero) for 0% C_{org}, indicating that the nitrogen in surface sediments was chiefly organic (Fig. 2). Surface sediment C_{org} contents ranged between 0.5 and 3.4% (average 1.9) and total nitrogen between 0.04 and 0.38% (average 0.18) (Fig. 3; Table 2), as shown in previous reports for the area (Silva et al., 1998a; Silva and Prego, 2002; Rojas and Silva, 2003). No clear trend in C_{org} and total nitrogen content was observed from the open ocean to inner fjord areas, although the lowest values occurred at stations (St.) 1, 27, 28, and 29 (Table 2), where sandy sediments and low

organic carbon content have been found previously (Silva et al., 1998a; Silva and Prego, 2002). No correlation was found between C_{org} and total nitrogen vs. water depth.

We used the N/C ratio instead of the C/N ratio because it has been demonstrated to more efficiently reflect the contribution of terrestrial organic carbon in marine environments (Perdue and Koprivnjak, 2007). The N/C ratio varied between 0.063 and 0.104 (average 0.082) and decreased from open ocean sediments to inner fjord areas, showing the lowest value near the Cisnes River in Puyuhuapi Fjord (St. 39; Figs. 1, 3). A similar trend was also found from the *Boca del Guafo* area to the head of Aysén Fjord (Rojas and Silva, 2003; Silva et al., this issue). Our N/C values are lower than those reported for open ocean sediments at 43° S (0.130 ± 0.003; Hebbeln et al., 2000) and are in the range of those found in other estuarine systems influenced by terrestrial organic matter contributions, including central and southern Patagonia (Table 3).

Suspended matter in the water column (5 m) ranged between 7.4 and 155 μg C_{org} L^{-1} (average 52) and between 1.1 and 27.4 μg nitrogen L^{-1} (average 8.0), resulting in a N/C ratio ranging between 0.089 and 0.171 (average 0.127), indicative of a strong marine component (Table 2). The N/C ratios were in the range of other estuarine and fjord systems (e.g., Goñi et al., 2003; Gašparović et al., 2005), although the C concentrations were comparatively lower than those reported for the upper 25 m of the water column in the same area (Gonzalez et al., this issue).

Riverine sediments (<125 μm) showed C_{org} values between 0.2 and 5.7% (average 1.7) and nitrogen values between 0.02 and 0.41% (average 0.12), resulting in a very narrow range of N/C (0.060–0.066, average 0.062) for all five rivers (Table 2). These N/C ratios were generally slightly lower than those reported for Chiloé Island and the Blanco River in Aysén Fjord (Silva et al., this issue), falling between those of typical C_3 land plants and

freshwater algae (Meyers, 1997) and within the range found for suspended particulate organic matter from rivers worldwide (Meybeck, 1982).

Degraded vegetation exhibited C_{org} and nitrogen contents ranging between 15.1 and 27.6% and 0.5 and 0.7%, respectively, whereas living terrestrial vegetation presented C_{org} values between 39.8 and 44.6% and nitrogen between 0.9 and 2.8% (Table 2). The N/C ratio in degraded vegetation varied between 0.018 and 0.058 (average 0.033), whereas the ratio for living vegetation fluctuated between 0.018 and 0.058 (Table 2); both were within the range reported for C_3 land vegetation (e.g., Meyers, 1997; Goñi et al., 2003 and references therein). Similar N/C values have been reported for other fresh plant species (0.025–0.039), degraded vegetation (0.016–0.020), and soils (0.024–0.064) from forests in the Chiloe Island National Park, Chile (42°30'S; Pérez, 1996), and from degraded vegetation around the Reloncaví and Aysén fjords (0.015–0.018; Silva et al., this issue). The wide range of N/C values found in the living vegetation reflected the variety of species analyzed, revealing the natural variation in the biochemical composition of land plants (e.g., Meyers, 2003).

3.2. Stable carbon and nitrogen isotope composition

A wide range of $\delta^{13}C$ values was found in surface sediments, varying between –28 and –19‰ and averaging –23.25 (Table 2; Fig. 3). Except for St. 39, which is located at the Cisnes River outlet (Fig. 1), sedimentary $\delta^{13}C$ values were generally higher than –25‰. $\delta^{15}N$ values varied between 1.4 and 9‰, with most of the samples displaying values above 6‰ (average 7‰). Strong gradients were observed for both $\delta^{13}C$ and $\delta^{15}N$, with values moving from enriched at open ocean sites to depleted at fjord heads and in areas of

restricted circulation (Table 2, Fig. 3). These gradients reflected increased contributions of terrestrial organic matter and are consistent with that of the N/C ratio (Fig. 3). The most depleted values, found at St. 39, could be the result of enhanced contributions of ^{13}C– and ^{15}N–depleted terrestrial organic matter from the Cisnes River (–27 and 0.7‰, respectively). The overall $\delta^{13}C$ signature of surface sediments in the Chilean fjord system is similar to that reported for fjords and river–dominated margins reported to have a marked mixing of marine and terrestrial C_{org} (Table 3).

$\delta^{13}C$ values of particulate organic matter ranged between –22.7 and –18.3‰ (average –20.7‰; Table 2; Fig. 3), and were generally more enriched than POM from a lake–river–fjord transect in central Patagonia (Vargas et al., this issue) and than surface waters of other fjords and estuarine systems (Goñi et al., 2005; McCallister et al., 2006; Velinsky and Fogel, 1999). Whereas the low $\delta^{13}C$ of particulate organic matter found in a permanently anoxic fjord in Norway was related to the presence of the green photo–autotrophic bacteria *Chlorobium* sp. (Velinsky and Fogel, 1999), in other estuarine areas this $\delta^{13}C$ has been associated with high contributions of organic matter from vascular plants (Goñi et al., 2005; McCallister et al., 2006). Our values are rather similar to those found for continental margins and open ocean areas (Table 3), indicating a strong marine component in the particulate organic matter of the Chilean fjords.

$\delta^{15}N$ values of particulate organic matter ranged between 7.7 and 11.5‰ (average 9.4; Table 2; Fig. 3). These values were similar to those in areas with a strong gradient from terrestrial to marine end–members such as Chesapeake Bay (McCallister et al., 2006) but heavier than in areas where high fractionation has been observed during nitrate uptake such as Framvaren Fjord, Norway (Velinsky and Fogel, 1999). In contrast to surface sediments,

no trend was observed between carbon and nitrogen isotopes in particulate organic matter from open ocean areas to the fjord heads (Fig. 3). Since our samples were collected at 5 m depth, we expected a dominant phytoplankton signature in suspended material consistent with the highest concentrations of chlorophyll occurring in the first 10 m of the water column during sampling (Rojas et al., 2005). To assess the effect of nutrient concentrations on phytoplankton fractionation during uptake, we compared our $\delta^{15}N$ of surface sediments and particulate organic matter with published nitrate concentrations for the top 5 m of the water column during the same sampling campaign (Rojas et al., 2005; data not displayed). No clear relation was found between nitrate and the $\delta^{15}N$ of the surface sediments (r^2 = 0.24) or the $\delta^{15}N$ of particulate organic matter (r^2 = 0.29). This observation suggests that sedimentary $\delta^{15}N$ most likely mirrors a mixture of marine and terrestrial organic matter sources instead of the isotope fractionation imprint of the assimilation of nitrate by phytoplankton in surface waters. The lack of the latter could be related to the highly heterogeneous distribution of phytoplankton in the area, which is controlled by local conditions of light penetration in the water column (Pizarro et al., 2005), and to the integrated signal of the top layer of the sediment. Since suboxic conditions have never been reported for the water column of this area, other processes like denitrification are not likely to occur in surface waters.

River sediments exhibited $\delta^{13}C$ and $\delta^{15}N$ values between –30 and –26.7‰ and between –1 and 2.4‰, respectively (Table 2). These values were similar to those reported by Silva et al. (this issue) for the Blanco River in Aysén Fjord but ^{13}C–depleted compared to POM from a lake–river–fjord transect in central Patagonia (Vargas et al., this issue), suggesting that most of the C_{org} carried by riverine sediments was derived predominantly from

terrestrial plants rather than freshwater phytoplankton. These values were also ^{13}C–depleted compared to sediments and POM in North America (Prahl et al., 1994; Onstad et al., 2000), likely due to the absence of C_4 plants in the study area.

Degraded vegetation showed $\delta^{13}C$ and $\delta^{15}N$ values between –29 and –28.5‰ and between –3.6 and –2‰, respectively, whereas fresh vegetation showed $\delta^{13}C$ and $\delta^{15}N$ values between –32 and –28‰ and between –4.3 and 6.7‰ (Table 2). Similar $\delta^{13}C$ values have been also described for degraded vegetation around the Relocaví and Aysén fjords (Silva et al., this issue). $\delta^{15}N$ values of fresh vegetation were in the range of global 'climosequence' patterns (Amundson et al., 2003). For both C and N isotopes, degraded vegetation was enriched compared with fresh vegetation (Table 2), likely due to microbial degradation (Lehmann et al., 2002). Both degraded and fresh vegetation $\delta^{13}C$ values were in the range of C_3 land plants (O'Leary, 1988; Meyers, 1997). Degraded vegetation displayed a narrower range of values than fresh vegetation (0.5 and 1.6‰ of difference for $\delta^{13}C$ and $\delta^{15}N$, respectively), which could reflect preferential degradation of the more isotopically depleted terrestrial debris by microbes in soil and rivers.

3.3. n–alkanoic fatty acid leaf waxes

The *n*–alkanoic fatty acids (FA) were present as C_{16} to C_{32} homologues (Fig. 4), with small concentrations of C_{34} in some areas. We focus on the long–chain (even–numbered C_{24}–C_{32}) *n*–alkanoic FAs, which are mainly derived from epicuticular leaf waxes of vascular plants (Eglinton and Hamilton, 1967; Meyers, 1997). Surface sediment concentrations of C_{24}–C_{32} *n*–alkanoic FAs varied between 1.6 and 29.0 μg gdw^{-1}, or 0.2 and 1.6 mg gC_{org}^{-1} (Table 2; Fig. 3). The lowest values (standardized to

organic carbon) were found at St. 1, where a marked marine influence is evident, whereas the highest concentrations were found toward the heads of the fjords (except for St. 28) and close to river outlets (i.e., St. 39, 40), in accordance with our elemental and isotopic data (Fig. 3). These elevated concentrations are comparable to values found in lacustrine sediments in Kenya (Huang et al., 1999) and are up to two orders of magnitude higher than in Norwegian fjord sediments (Smittenberg et al., 2004) and the open ocean off northwest Africa (Huang et al., 2000). Station 28 showed lower FA concentrations than expected considering its location (Fig. 1). This anomaly may be the result of dilution by fine sediments resulting from glacial erosion due to the proximity of the Northern Ice Fields (*Campos de Hielo Norte*). Furthermore, the vegetation surrounding the Cupquelan Fjord near the Northern Ice Fields is mostly composed of Andean tundra rather than forest (Gajardo, 1994; Veblen et al., 1997).

FA concentrations in river sediments varied between 0.2 and 0.8 mg gC_{org}^{-1}, whereas degraded vegetation presented values below or equal to 0.02 mg g C_{org}^{-1} (Table 2). The FA concentration in fresh vegetation varied between 0.01 and 1.4 mg g C_{org}^{-1}, with the highest values found in the tree *Nothofagus* sp. and two species of understory shrubs: *Libertia chilensis* and *Scirpus* sp. The rest of the vegetation exhibited values lower than 0.2 mg gC_{org}^{-1} (Table 2). The average FA concentration in fresh vegetation was twice as high as in degraded vegetation (Table 2), most likely due to the physical removal of leaves and dilution with wood remains in soil and rivers.

FAs in surface sediments displayed an even–over–odd predominance as indicated by their CPI values (range 2.8 and 4.2, average 3.4; Table 2; Fig. 3). This configuration reflected the land–plant source and limited degradation of the FAs

(Eglinton and Hamilton, 1967). The *n*–alkanoic acid distribution of homologues in surface sediments was bimodal in shape, peaking at *n*–C_{28} and *n*–C_{16}, with *n*–C_{28} being generally more prominent (Fig. 4). The *n*–alkanoic acids in riverine sediments resembled the bimodal distribution observed in fjord sediments, except for the Condor River, which showed similar contributions of the *n*–$C_{16–22–24–26–28}$ homologues (Fig. 4). Degraded vegetation showed the predominance of homologues shorter than *n*–C_{22}, peaking at *n*–C_{16} and *n*–C_{22} (Fig. 4). Fresh land vegetation displayed a very heterogeneous distribution of *n*–alkanoic acids without a common pattern of carbon–number predominance on chains above *n*–C_{24}. Except for tree species, most of the vegetation was enriched in *n*–C_{16} (between 40 and 85% dominance; Fig. 4). Since leaves from fresh vegetation were completely ground before analysis, the homologue distribution may also have included the distribution of short–chain fatty acids present in cuticular and subcuticular leaf cells. In surface sediments (excluding St. 39), all homologues (except for *n*–C_{16}) showed a distribution similar to that found in the tree *Nothofagus* (Fig. 4). *Nothofagus* may be considered to be the main source of long–chain FAs in this area since it has been described as the dominant and most broadly distributed genus in the northern Patagonian rainforest (Arroyo et al., 1997). FAs obtained from POM in a lake–river–fjord corridor in Central Patagonia were dominated by short–chain homologues (*n*–C_{16} and *n*–C_{18}) of planktonic origin, whereas a high proportion of long–chain homologues of terrestrial origin was found in rivers (Vargas et al., this issue).

ACL in the surface sediments varied between 25.4 and 28.2, and most of the stations presented values above 27 (Table 2; Fig. 3). ACL in river sediments (<125–μm fraction) varied between 26.8 and 27.4, whereas degraded vegetation exhibited

values between 26 and 26.8. Fresh vegetation displayed the widest range of ACL (25.4–29.4), reflecting the diversity of the studied plants (grasses, ferns, bushes, trees), of which the grasses had the highest values (Table 2; Fig. 3). ACL has been shown to increase equatorward in response to decreased humidity and increased temperature, possibly as a protection against water loss (Sachse et al., 2006). ACL has also been used to assess variations in precipitation and humidity over the last two millennia in northern Patagonia (Sepúlveda et al., 2009). No clear trend was observed with station location (Fig. 3), indicating similarity of the vegetation, which was dominated largely by *Nothofagus* sp. and *Podocarpus* sp. (Gajardo, 1994). Slightly higher ACL values were found at St. 1 and 6 (27.8 and 28.2, respectively). Since these stations are located in the northernmost fjord area and close to the open ocean influence, eolian transport from northern and less humid areas could possibly explain the presence of slightly higher ACL values. Due to the high annual precipitation (up to 3,000 mm y^{-1}; DGA, 2003), a contribution from C_4 plants was not expected. Low ACL values were found in degraded vegetation (26–26.8; Table 2, Fig. 3), likely as a result of non–selective degradation.

3.4. Autochthonous and allochthonous organic matter sources

We obtained our marine end–member values for $\delta^{13}C$, $\delta^{15}N$, and N/C by averaging those from St. 1 (outside the fjord area and within typical marine values) and those obtained by Hebbeln et al. (2000) from surface sediments of the continental slope off Chile (41° S–43°13'S; Table 2). The terrestrial end–member was obtained as the average of three different pools: a) the <125–µm fraction from river surface sediments, b) degraded

vegetation carried by rivers, and c) fresh terrestrial vegetation (Table 2). Marine and terrestrial end–members were statistically different and all values were within the range described for other coastal environments (Tables 2, 3).

By plotting the elemental and isotopic composition of both end–member components together with surface sediments from the fjord system, the best linear regression fit was between $\delta^{13}C$ and N/C ratio ($r^2 = 0.85$; Fig. 5). We used the N/C ratio instead of the C/N ratio because it better represents the fraction of terrestrially derived organic carbon (Perdue and Koprivnjak, 2007). The linearity of our data suggests that nearly all of the organic carbon delivered to the surface sediments in the northern Patagonia fjord system was mixed, from two main sources: marine and terrestrial. However, the presence of allochthonous anthropogenic sources from wastewaters and salmon farming, reported to be discernible in sediments surrounding cages in shallow inner seas between 41° and 45°30' S (Soto and Norambuena, 2004), cannot be ruled out. Salmon farming is known to promote geochemical and ecological changes in aquatic ecosystems (e.g., Johannessen et al., 1994; Morrisey et al., 2000), and the waste material from fish farming can be traced as far as 1,000 m from cages in shallow areas (e.g., Sarà et al., 2004). However, reported $\delta^{13}C$ and $\delta^{15}N$ values for pellet feed (–22.7 ± 1.1 and 8.3 ± 2.1‰; Sarà et al., 2004) are close to our marine end–member, whereas the $\delta^{13}C$ and $\delta^{15}N$ from farmed fish feces (–21.0 ± 0.1 and 10.6 ± 0.3‰; Sarà et al., 2004) fall between our marine and terrestrial end–members (Fig. 5; Table 2), complicating an accurate estimation of the contribution of salmon farming to sedimentary organic matter in this region with this technique.

3.5. Mixing of organic matter sources

We calculated the contribution of marine and terrestrial sources to the organic carbon pool in surface sediments using a mixing equation (e.g., Thornton and McManus, 1994; Schlünz et al., 1999):

$$\int_M = [\delta^{13}C_i - \delta^{13}C_T] / [\delta^{13}C_M - \delta^{13}C_T] \quad \text{(Eq. 1)}$$

$$\int_T = 1 - \int_M \quad \text{(Eq. 2)}$$

where $\int_M$ = marine fraction of C_{org}, $\delta^{13}C_i = \delta^{13}C$ of a given sample, $\delta^{13}C_T = \delta^{13}C$ of the terrigenous end–member, $\delta^{13}C_M = \delta^{13}C$ of the marine end–member, and $\int_T$ = terrigenous fraction of C_{org}. Mixing was estimated from the $\delta^{13}C$ data since this proxy is carbon–normalized. The proportion of marine C_{org} ($C_{org–m}$) in the inner fjords (except for St. 39, located at the mouth of the Cisnes River; 13%) varied between 42 and 97% (Fig. 6). As expected, a trend of increased terrestrial C_{org} ($C_{org–t}$) from 3 to 87% was observed from St. 6 to those sites located within the inner fjords and close to river mouths, following the characteristic salinity gradient of this area (Fig. 6; Silva et al., 1997, 1998b). A similar trend has also been observed previously from the mouth of Moraleda Chanel to the head of Aysén Fjord (Pinto and Bonert, 2005; Silva et al., this issue).

3.6. Organic carbon burial rates and CO_2 sequestration

We calculated a C_{org} accumulation rate (C_{org}AR) ranging between 0.7 and 82.5 g C m^{-2} yr^{-1} at the sediment–water interface of the study area (blue and green areas in Fig. 1a) by integrating our results with published data (C_{org} content, sedimentation rate, and porosity, ~44–47º S; Table 4). A sediment dry density of 1.85 g cm^{-3} is assumed for the entire region (Pantoja et al., 2009). Although only a few data points are available, post–depositional burial efficiencies in recent sediments (~30 cm) of northern Patagonia have been estimated

to vary between 63% for Puyuhuapi Fjord (Sepúlveda et al., 2005), 65 to 77% for Moraleda Channel, and 78 to 89% for Aysén Fjord and Costa Channel (Rojas and Silva, 2005). Thus, a conservative C_{org} burial rate of 0.4 to 52 g C/m^2 yr can be obtained by using the lowest burial efficiency reported for this area (63%; Sepúlveda et al., 2005), resulting in C_{org} burial between 2.3 and 7.8 x 10^4 ton yr^{-1} for the entire study area (Fig. 1a; Table 4). These values are maximum estimates since diagenetic changes below 30 cm are not considered and are in the same range as other high–latitude fjords and shelf seas in the Northern Hemisphere such as the eastern Canadian Margin (Muzuka and Hillaire–Marcel, 1999; St–Onge and Hillaire–Marcel, 2001) and the Storfjord area of Spitbergen (Winkelmann and Knies, 2005) (Table 4).

Subsequently, by extrapolating the proportion of $C_{org–m}$ for each individual fjord, obtained from the mixing model and our local marine and terrestrial end–members, and using published data for the Moraleda Channel (Silva et al., this issue), we calculate a $C_{org–m}$ flux at the sediment surface between 0.3 and 40.2 g C m^{-2} yr^{-1} (Table 4). Thus, the calculated $C_{org–m}$ burial (0.2–25.3 g C m^{-2} yr^{-1}) equaled between 1.8 and 6.2 x 10^4 ton C yr^{-1} for the entire study area. In contrast, the burial of $C_{org–t}$ delivered by rivers and continental runoff accounted for between 0.5 and 1.6 x 10^4 ton C yr^{-1} (obtained as the difference between C_{org} and $C_{org–m}$ burial).

Primary production in northern Patagonia during spring and summer months ranged between 0.23 and 5.16 g C m^{-2} d^{-1}, and between 1.42 and 4.38 g C m^{-2} d^{-1}, respectively (Aracena et al., this issue; González et al., this issue). Thus, an integrated rate of 311 ± 293 g C m^{-2} y^{-1}, equivalent to 1.3 x 10^6 ± 1.2 x 10^6 ton C yr^{-1}, was calculated for the entire study area (~ 4,280 km^2). We assumed that marine productivity in spring/summer dominated the yearly export of organic matter to surface sediments. The latter is based on

the low productivity (~ 2 mg C m^{-2} h^{-1}; Pizarro et al., 2005) and low vertical C_{org} export (González et al., this issue), in addition to evidence suggesting that most of the organic carbon is rapidly recycled by bacteria (Montero et al., this issue) during the non–productive season (autumn/winter). Thus, our calculated $C_{org–m}$ burial represented between 1 and 4% of the photosynthetic carbon fixation in the surface waters, indicating than more than 96% was mineralized and/or advected within the water column.

Based on the stoichiometry of photosynthesis, in which 1 gram of $C_{org–m}$ ultimately derives from 3.6 grams of CO_2, our calculations of $C_{org–m}$ burial equaled an atmospheric CO_2 sequestration between 0.06 and 0.23 x 10^6 ton CO_2 yr^{-1} (or 15.3 to 53.1 tons CO_2/km^2) for the studied area (Table 5). Despite the natural variability of this system (Aracena et al., this issue; González et al., this issue) and large range of values accompanying these calculations, these results are in accordance with recent evidence indicating that surface waters in the Patagonian fjord system are undersaturated with respect to CO_2 and therefore act as a CO_2 sink (R. Torres, pers. comm.). It is important to clarify that our calculations only include the fixation of inorganic carbon into organic carbon during photosynthesis and do not consider the role of calcifying planktonic organisms. However, the average inorganic carbon content in surface sediments from the study area was rather low (~ 0.4% in the inner fjords and ~ 0.05% in the southern area of northern Patagonia; Silva and Prego, 2002), suggesting that the contribution of the inorganic carbon pump in CO_2 sequestration is rather small. To place these results into a larger context, the CO_2 sequestration calculated for the northern Patagonia fjord system represented between 0.4 and 1.5 % of Chile's fossil fuel CO_2 emissions in 2001 (15 x 10^6 metric tons; Marland et al., 2007); this range is similar range to calculations reported for the Storfjorden in Spitsbergen (0.28–0.90 x 10^6 ton CO_2 yr^{-1} or 19.6–63.1 tons CO_2/km^2; Winkelmann and Knies, 2005; Table 5).

However, if we consider that the entire Patagonian fjord area from the city of Puerto Montt (42˚30'S) to Cape Horn (55˚58'S) encompasses almost 240,000 km^2 (Silva and Prego, 2002), our study suggests that the Chilean fjord system can potentially act as an important region for C_{org} burial and as a CO_2 sink.

4. Concluding remarks

We aimed to characterize the geochemistry of surface sediments from the northern Patagonia fjord system and to identify the mixing of marine and terrestrial organic carbon sources in order to better constrain C_{org} cycling in an area that may be impacted by the effects of expanding economic development. This study also provides a basis for future studies focusing on past environmental and/or climate changes using sedimentary sequences in Patagonia.

Averaged geochemical values for end–members in the study area were N/C 0.127 ± 0.010, $\delta^{13}C$ –19.8 ± 0.3‰, and $\delta^{15}N$ 9.9 ± 0.5‰ for marine organic matter, and N/C 0.040 ± 0.018, $\delta^{13}C$ –29.3 ± 2.1‰, and $\delta^{15}N$ 0.2 ± 3.0‰ for terrestrial organic matter. Based on these end–member values, we assessed the contribution of marine and terrestrial organic carbon sources in the marine/estuarine system. Marine–derived organic carbon accounted for about 13 to 96% of the total in surface sediments, whereas terrestrial organic carbon represented the remainder of the pool. A strong gradient (84% difference) of organic carbon sources was found between open ocean areas and those located in more restricted and isolated settings at the heads of fjords and close to river outlets. This gradient was paralleled by the surface sediment concentration of long–chain *n*–alkanoic FAs derived from the epicuticular leaf waxes of vascular plants, which increased towards the heads of

the fjords and near river outlets. The homologous distribution of *n*–alkanoic FAs in surface sediments suggests that the genus *Nothofagus* may be the most important source of these FAs in the area, consistent with the broad distribution of this genus in the northern Patagonian rainforest.

The relationship between nitrate in surface waters and nitrogen isotopes in particulate organic carbon and surface sediments indicated that neither of the last two reflects the processes involved in nutrient assimilation by phytoplankton during photosynthesis, but rather the mixture of marine and terrestrial organic matter.

Integrated regional calculations in sediments from the northern Patagonia fjord system (~4,280 km^2) suggested that the sequestration of marine phytoplanktonic C_{org} from surface waters may account for between 1.8 and 6.2 x 10^4 ton C yr^{-1}, representing an assimilation of CO_2 by photosynthesis between 0.06 and 0.23 x 10^6 ton yr^{-1}. Despite the large range of values accompanying these calculations, our results suggest that the Chilean fjord system of Patagonia may be a potentially important area for the burial of marine C_{org} and as a CO_2 sink.

Acknowledgments

We thank the National Hydrographic and Oceanographic Service of the Chilean Navy (SHOA), the captain and crew of the AGOR Vidal Gormaz for their professional help during the CIMAR FIORDO 7 fieldwork, and the EULA Center, University of Concepción (UDEC), for logistical support. We also thank C. Bertrand, N. Drenzek, D. Montlucon, and L. Xu for laboratory assistance; M. Negrito for the vegetation taxonomy; S. Bertrand for fruitful discussion and access to the map used in Fig. 1; P. Vera for logistical assistance before and during the cruise; and D. Barriga for editorial comments. Three anonymous

reviewers are acknowledged for their constructive comments. J. Sepúlveda was funded by a M.S. scholarship from the Graduate School at UDEC and by Fundación Andes through the Woods Hole Oceanographic Institution (WHOI)/UDEC agreement during a research visit at WHOI. This research was funded by the Ministerio de Hacienda de Chile and the Comité Oceanográfico Nacional (CONA) through the CIMAR–7 FIORDO Program (Grant C7F 01–10 to SP), CONICYT/NSF Grant 2001–120, Fundación Andes–Chile, and the Center for Oceanographic Research in the eastern South Pacific (COPAS) and COPAS Sur–Austral (PFB–31/2007).

References

Amundson, R., Austin, A.T., Schuur, E.A.G., Yoo, K., Matzek, V., Kendall, C., Uebersax, A., Brenner, D., Baisden, W.T., 2003. Global patterns of the isotopic composition of soil and plant nitrogen. Global Biogeochem. Cy. 17, doi:10.1029/2002GB001903.

Aracena, C., Lange, C., Iriarte, J.L., Rebolledo, L., Pantoja, S., this issue. Latitudinal patterns of export production recorded in surface sediments of the Chilean Patagonian fjords (41–55° S) as a response to water column productivity. Cont. Shelf Res.

Araya, J.F., 1997. Perfiles geomorfológicos de los fiordos y depresión longitudinal de norpatagonia. Ciencia y Tecnología del Mar 20, 3–20.

Arroyo, M., Cavieres, L., Peñaloza, A., Riveros, M., Faggi, M., 1997. Relaciones fitogeográficas y patrones de riqueza de especies en la flora del bosque lluvioso templado de Sudamérica, in: Armesto, J., Villagrán, C., Arroyo, M., (Eds.), Ecología de los bosques nativos de Chile. Editorial Universitaria, Santiago, pp. 71–99.

Borgel, R., 1970. Geomorfología de las regiones australes de Chile. Revista Geográfica de Chile 'Terra Australis' 20, 135–140.

Cranwell, P.A., 1981. Diagenesis of free and bound lipids in terrestrial detritus deposited in a lacustrine sediment. Org. Geochem. 3, 79–89.

DaSilva, J.L., Anderson, J.B., Stravers, J., 1997. Seismic facies changes along a nearly continuous 24° latitudinal transect: the fjords of Chile and the northern Antarctic Peninsula. Mar. Geol. 143, 103–123.

Dávila, P.M., Figueroa, D., Müller, E., 2002. Freshwater input into the coastal ocean and its relation with the salinity distribution off austral Chile (35–55°S). Cont. Shelf Res. 22, 521–534.

de Haas, H., van Weering, T.C.E., de Stigter, H., 2002. Organic carbon in shelf seas: sinks or sources, processes and products. Cont. Shelf Res. 22, 691–717.

Delgado, S., 2004. Relación entre el perfil del basamiento de fiordos y canales y la morfoestructura regional en Norpatagonia. Tesis para optar al grado de Magíster en Geografía con mención en Evaluación Territorial, University of Chile, Santiago.

DGA, 2003. Dirección General de Aguas, Chile (http://www.dga.cl).

Eglinton, G., Hamilton, R.J., 1967. Leaf epicuticular waxes. Science 156, 1322–1335.

Freudenthal, T., Wagner, T., Wenzhöfer, F., Zabel, M., Wefer, G., 2001. Early diagenesis of organic matter from sediments of the eastern subtropical Atlantic: evidence from stable nitrogen and carbon isotopes. Geochim. Cosmochim. Acta 65, 1795–1808.

Gajardo, R., 1994. La vegetación natural de Chile, clasificación y distribución geográfica. Editorial Universitaria, Santiago.

Gašparović, B., Plavsic, M., Cosovic, B., Reigstad, M., 2005. Organic matter characterization and fate in the sub–arctic Norwegian fjords during the late spring/summer period. Estuar. Coast. Shelf Sci. 62, 95–107.

González, H.E., Castro, L., Daneri, G., Iriarte, J.L., Silva, N., Vargas, C., Giesecke, R., Sánchez, N., this issue. Seasonal plankton variability in Chilean Patagonia Fjords: carbon flow through the pelagic food web of the Aysen Fjord and plankton dynamics in the Moraleda Channel basin. Cont. Shelf Res.

Goñi, M.A., Cathey, M.W., Kim, Y.H., Voulgaris, G., 2005. Fluxes and sources of suspended organic matter in an estuarine turbidity maximum region during low discharge conditions. Estuar. Coast. Shelf Sci. 63, 683–700.

Goñi, M.A., Teixeira, M.J., Perkey, D.W., 2003. Sources and distribution of organic matter in a river–dominated estuary (Winyah Bay, SC, USA). Estuar. Coast. Shelf Sci. 57, 1023–1048.

Haddad, R.I., Martens, C.S., Farrington, J.W., 1992. Quantifying early diagenesis of fatty acids in a rapidly accumulating coastal marine sediment. Org. Geochem. 19, 205–216.

Hebbeln, D., Marchant, M., Freudenthal, T., Wefer, G., 2000. Surface sediment distribution along the Chilean continental slope related to upwelling and productivity. Mar. Geol. 164, 119–137.

Hedges, J.I., Keil, R.G., 1995. Sedimentary organic matter preservation: an assessment and speculative synthesis. Mar. Chem. 49, 81–115.

Huang, Y., Dupont, L., Sarnthein, M., Hayes, J.M., Eglinton, G., 2000. Mapping of C_4 plant input from North West Africa into North East Atlantic sediments. Geochim. Cosmochim. Acta 64, 3505–3513.

Huang, Y., Street–Perrott, F.A., Perrott, R.A., Metzger, P., Eglinton, G., 1999. Glacial–interglacial environmental changes inferred from molecular and compound–specific $\delta^{13}C$ analyses of sediments from Sacred Lake, Mt. Kenya. Geochim. Cosmochim. Acta 63, 1383–1404.

Hughen, K.A., Eglinton, T.I., Xu, L., Makou, M., 2004. Abrupt tropical vegetation response to rapid climate changes. Science 304, 1955–1959.

Johannessen, P.J., Botnen, H.B., Tvedten, Ø., 1994. Macrobenthos: before, during and after a fish farm. Aquaculture and Fisheries Management 25, 55–66.

Lehmann, M.F., Bernasconi, S.M., Barbieri, A., McKenzie, J.A., 2002. Preservation of organic matter and alteration of its carbon and nitrogen isotope composition during simulated and in situ early sedimentary diagenesis. Geochim. Cosmochim. Acta 66, 3573–3584.

Logan, G.A., Smiley, C.J., Eglinton, G., 1995. Preservation of fossil leaf waxes in association with their source tissues, Clarkia, northern Idaho, USA. Geochim. Cosmochim. Acta 59, 751–763.

Louchouarn, P., Lucotte, M., Canuel, R., Gagné, J.P., Richard, L.P., 1997. Sources and early diagenesis of lignin and bulk organic matter in the sediments of the Lower St. Lawrence Estuary and the Saguenay Fjord. Mar. Chem. 58, 3–26.

Maksymowska, D., Richard, P., Piekarek–Jankowska, H., Riera, P., 2000. Chemical and isotopic composition of the organic matter sources in the Gulf of Gdansk (Southern Baltic Sea). Estuar. Coast. Shelf Sci. 51, 585–598.

Marland, G., Boden, T.A., Andres, R.J., 2007. Global, Regional, and National CO2 Emissions. Trends: A Compendium of Data on Global Change. Nature Publishing Group.

Mayer, L.M., 1994a. Relationships between mineral surfaces and organic carbon in soils and sediments. Chem. Geol. 114, 347–363.

Mayer, L.M., 1994b. Surface area control of organic carbon accumulation in continental shelf sediments. Geochim. Cosmochim. Acta 58, 1271–1284.

McCallister, S.L., Bauer, J.E., Ducklow, H.W., Canuel, E.A., 2006. Sources of estuarine dissolved and particulate organic matter: A multi–tracer approach. Org. Geochem. 37, 454–468.

Meybeck, M., 1982. Carbon, nitrogen, and phosphorus transport by world rivers. Am. J. Sci. 282, 401–450.

Meyers, P.A., 1994. Preservation of elemental and isotopic source identification of sedimentary organic matter. Chem. Geol. 114, 289–302.

Meyers, P.A., 1997. Organic geochemical proxies of paleoceanographic, paleolimnologic, and paleoclimatic processes. Org. Geochem. 27, 213–250.

Meyers, P.A., 2003. Applications of organic geochemistry to paleolimnological reconstructions: a summary of examples from the Laurentian Great Lakes. Org. Geochem. 34, 261–289.

Montero, P., Daneri, G., González, H.A., Iriarte, J.L. Tapia, F.J., Lizárraga, L., Sanchez, N., Pizarro, O., this issue. Seasonal variability of primary production in a fjord ecosystem of the Chilean Patagonia: implications for the transfer of carbon within pelagic food webs. Cont. Shelf Res.

Morrisey, D.J., Gibbs, M.M., Pickmere, S.E., Cole, R.G., 2000. Predicting impacts and recovery of marine–farm sites in Stewart Island, New Zealand, from the Findlay–Watling model. Aquaculture 185, 257–271.

Muller–Karger, F.E., Varela, R., Thunell, R., Luerssen, R., Hu, C., Walsh, J.J., 2005. The importance of continental margins in the global carbon cycle. Geophys. Res. Lett. 32, 10.1029/2004gl021346.

Müller, A., 2001. Geochemical expressions of anoxic conditions in Nordåsvannet, a land–locked fjord in western Norway. Appl. Geochem. 16, 363–374.

Muzuka, A., Hillaire–Marcel, C., 1999. Burial rates of organic matter along the eastern Canadian margin and stable isotope constraints on its origin and diagenetic evolution. Mar. Geol. 160, 251–270.

O'Leary, M.H., 1981. Carbon isotope fractionation in plants. Phytochemistry 20, 553–568.

O'Leary, M.H., 1988. Carbon isotopes in photosynthesis. Bioscience, 328–336.

Ohkouchi, N., Kawamura, K., Kawahata, H., Taira, A., 1997. Latitudinal distributions of terrestrial biomarkers in the sediments from the Central Pacific. Geochim. Cosmochim. Acta 61, 1911–1918.

Onstad, G.D., Canfield, D.E., Quay, P.D., Hedges, J.I., 2000. Sources of particulate organic matter in rivers from the continental USA: lignin phenol and stable carbon isotope compositions. Geochim. Cosmochim. Acta 64, 3539–3546.

Pantoja, S., Iriarte, J.L., Gutiérrez, M., Calvete, C., 2009. The Southern Chile Continental Margin, in: Liu, K.K., Atkinson, L., Quiñones, R.A., Talaue–McManus, L. (Eds.), Carbon and nutrient fluxes in continental margins. Springer, Berlin, pp. 265–273.

Perdue, E.M., Koprivnjak, J–F., 2007. Using the C/N ratio to estimate terrigenous inputs of organic matter to aquatic environments. Estuar. Coast. Shelf Sci. 73, 65–72.

Pérez, C.A., 1996. Litter decomposition processes in coastal temperate forests: Interactions between plants, soils, and vegetation, in: Armesto, J.J., Villagrán, C., Arroyo, M.K. (Eds.), Ecología de los Bosques Nativos de Chile. Editorial Universitaria, Santiago, pp. 301–315.

Peters, K.E., Sweeney, R.E., Kaplan, I.R., 1978. Correlation of carbon and nitrogen stable isotope ratios in sedimentary organic matter. Limnol. Oceanogr. 23, 598–604.

Pickard, G.L., 1971. Some physical oceanographic features of inlets of Chile. J. Fish. Res. Board Can. 28, 1077–1106.

Pickard, G.L., Stanton, B.R., 1980. Pacific fjords: a review of their water characteristics. Plenum Press, New York.

Pinto, L., Bonert, C., 2005. Origen y distribución de hidrocarburos alifáticos en sedimentos de Seno Aysén y Canal Moraleda, Chile austral. Ciencia y Tecnología del Mar 28, 35–44.

Pizarro, G., Astoreca, R., Montecinos, V., Paredes, M.A., Alarcón, G., Uribe, P., Guzmán, L., 2005. Patrones espaciales de la abundancia de la clorofila, su relación con la productividad primaria y la estructura de tamaños del fitoplancton en Julio y Noviembre de 2001 en la región de Aysén (43°–46° S). Ciencia y Tecnología del Mar 28, 27–42.

Prahl, F.G., Ertel, J.R., Goñi, M.A., Sparrow, M.A., Eversmeyer, B., 1994. Terrestrial organic carbon contributions to sediments on the Washington margin. Geochim. Cosmochim. Acta 58, 3035–3048.

Rojas, N., 2002. Distribución de materia orgánica, carbono y nitrógeno, y diagénesis temprana en sedimentos de la zona de canales australes entre los golfos Corcovado y Elefantes, Chile. Tesis para optar al título de Oceanógrafo, Universidad Católica de Valparaíso, Valparaíso.

Rojas, N., Silva, N., 2003. Distribución espacial de textura, C y N en sedimentos recientes en canales y fiordos chilenos. Golfo Corcovado (43º50’S) a golfo Elefantes (46º30’S), Chile. Ciencia y Tecnología del Mar 26, 15–31.

Rojas, N., Silva, N., 2005. Early diagenesis and vertical distribution of organic carbon and total nitrogen in recent sediments from southern Chilean fjords (Boca del Guafo to Pulluche Channel). Investigaciones Marinas 33, 183–194.

Rojas, R., Calvete, C., Otarola, G., Guerra, D., Silva, N., 2005. CD–ROM with data report from the Crucero Oceanográfico CIMAR 7 Fiordos. Centro Nacional de Datos Hidrográficos y Oceanográficos de Chile. Servicio Hidrográfico y Oceanográfico de la Armada, Chile.

Sachse, D., Radke, J., Gleixner, G., 2006. δD values of individual n–alkanes from terrestrial plants along a climatic gradient – Implications for the sedimentary biomarker record. Org. Geochem. 37, 469–483.

Salamanca, M.A., Jara, B., 2003. Distribución y acumulación de plomo (Pb y ^{210}Pb) en sedimentos de los fiordos de la XI región de Chile. Ciencia y Tecnología del Mar 26, 61–71.

Sarà, G., Scilipoti, D., Mazzola, A., Modica, A., 2004. Effects of fish farming waste to sedimentary and particulate organic matter in a southern Mediterranean area (Gulf of Castellammare, Sicily): a multiple stable isotope study δ^{13}C and δ^{15}N). Aquaculture 234, 199–213.

Schlünz, B., Schneider, R., Muller, P., Showers, W., Wefer, G., 1999. Terrestrial organic carbon accumulation on the Amazon deep sea fan during the last glacial sea level low stand. Chem. Geol. 159, 263–281.

Sepúlveda, J., Pantoja, S., Hughen, K., Lange, C., González, F., Muñoz, P., Rebolledo, L., Castro, R., Contreras, S., Ávila, A., Rossel, P., Lorca, G., Salamanca, M., Silva, N., 2005. Fluctuations in export productivity over the last century from sediments of a southern Chilean fjord (44°S). Estuar. Coast. Shelf Sci. 65, 587–600.

Sepúlveda, J., Pantoja, S., Hughen, K.A., Bertrand, S., Figueroa, D., León, T., Drenzekc, N.J., Lange, C., 2009. Late Holocene sea–surface temperature and precipitation variability in northern Patagonia, Chile (Jacaf Fjord, 44°S). Quaternary Res., doi:10.1016/j.yqres.2009.1006.1010.

Silva, N., Calvete, C., Sievers, H.A., 1997. Características oceanográficas físicas y químicas de canales australes Chilenos entre Puerto Montt y Laguna San Rafael (crucero CIMAR–FIORDO 1). Ciencia y Tecnología del Mar 20, 23–106.

Silva, N., Maturana, J., Sepúlveda, J.I., Ahumada, R., 1998a. Materia orgánica, C y N, su distribución y estequiometría, en sedimentos superficiales de la región norte de los fiordos y canales australes de Chile (crucero CIMAR–FIORDO 1). Ciencia y Tecnología del Mar 21, 49–74.

Silva, N., Calvete, C., Sievers, H.A., 1998b. Masas de agua y circulación general para algunos canales australes entre Puerto Montt y Laguna San Rafael, Chile (Crucero CIMAR–FIORDO 1). Ciencia y Tecnología del Mar 21, 17–48.

Silva, N., Haro, J., Prego, R., 2009. Metals background and enrichment in the Chiloé Interior Sea sediments (Chile). Is there any segregation between fjords, channels and sounds? Estuar. Coast. Shelf Sci. 82, 469–476.

Silva, N., Prego, R., 2002. Carbon and nitrogen spatial segregation and stoichiometry in the surface sediments of southern Chilean inlets (41°–56°S). Estuar. Coast. Shelf Sci. 55, 763–775.

Silva, N., Sievers, H., Prado, R., 1995. Caracteristicas oceanográficas y una proposición de circulación para algunos canales australes de Chile entre 41°20'S y 46°40'S. Revista de Biología Marina 30, 207–254.

Silva, N., Vargas, C.A., Prego, R., this issue. Land–ocean distribution of allochtonous organic matter in the surface sediments of the Chiloé and Aysén Interior Seas (Chilean Northern Patagonia). Cont. Shelf Res.

Silverberg, N., Sundby, B., Mucci, A., Zhong, S., Arakaki, T., Hall, P., Landén, A., Tengberg, A., 2000. Remineralization of organic carbon in eastern Canadian continental margin sediments. Deep–Sea Res. Pt. II: Topical Studies in Oceanography 47, 699–731.

Smittenberg, R.H., Pancost, R.D., Hopmans, E.C., Paetzel, M., Sinninghe Damsté, J.S., 2004. A 400–year record of environmental change in an euxinic fjord as revealed by the sedimentary biomarker record. Palaeogeogr. Palaeocl. Palaeoecol. 202, 331–351.

Soto, D., Norambuena, F., 2004. Evaluation of salmon farming effects on marine systems in the inner seas of southern Chile: a large–scale mensurative experiment. J. Appl. Ichthyol. 20, 493–501.

St–Onge, G., Hillaire–Marcel, C., 2001. Isotopic constraints of sedimentary inputs and organic carbon burial rates in the Saguenay Fjord, Quebec. Mar. Geol. 176, 1–22.

Thornton, S.F., McManus, J., 1994. Application of organic carbon and nitrogen stable isotope and C/N ratios as source indicators of organic matter provenance in estuarine systems: evidence from the Tay Estuary, Scotland. Estuar. Coast. Shelf Sci. 38, 219–233.

Vargas, C.A., Martinez, R.A., San Martina, V., Aguayo, M., Silva, N., Torres, R., this issue. Allochthonous subsidies of organic matter across a lake–river–fjord landscape in the Chilean Patagonia: implications for marine plankton food webs. Cont. Shelf Res.

Veblen, T., Kitzberger, T., Burns, B., Rebertus, A., 1997. Perturbaciones y dinámica de regeneración en bosques andinos del sur de Chile y Argentina, in: Armesto, J., Villagrán, C., Arroyo, M., (Eds.), Ecología de los bosques nativos de Chile. Editorial Universitaria, Santiago, pp. 169–198.

Velinsky, D.J., Fogel, M.L., 1999. Cycling of dissolved and particulate nitrogen and carbon in the Framvaren Fjord, Norway: stable isotopic variations. Mar. Chem. 67, 161–180.

Villagrán, C., 1988. Late quaternary vegetation of southern Isla Grande de Chiloé, Chile. Quaternary Res. 29, 294–306.

Winkelmann, D., Knies, J., 2005. Recent distribution and accumulation of organic carbon on the continental margin west off Spitsbergen. Geochem. Geophys. Geosys. 6, doi:10.1029/2005GC000916.

Zimmerman, A., Canuel, E., 2001. Bulk organic matter and lipid biomarker composition of Chesapeake Bay surficial sediments as indicators of environmental processes. Estuar. Coast. Shelf Sci. 53, 319–341.

Figure captions

Figure 1. Location of the sampling area in northern Patagonia (a) along the Chilean coast of South America (inset); the areas used for budget calculations are in green (geochemical data from this study) and blue (geochemical data from Silva et al., this issue; see text for details). (b) Enlargement showing the location of sampling sites for surface sediment (yellow circles), particulate organic matter (blue circles), fresh vegetation (green circles), and riverine sediments and degraded vegetation (red circles). White circles display stations for which C_{org} and/or $\delta^{13}C$ data were obtained from elsewhere (Pinto and Bonert, 2005; Silva et al., 1998a; Silva et al., this issue; see text for details). White numbers (except for those in Moraleda Channel) are according to Silva et al. (1998a). Main rivers are abbreviated as Aldunate (AR), Ventisquero (VR), Queulat Creek (QC), Cisnes (CR), Cuervo (CuR), Condor (CoR), and Aysén (AyR). Other locations described in the text and tables are also shown.

Figure 2. Regression between organic carbon (C_{org}) and total nitrogen (TN) in surface sediments.

Figure 3. Geochemistry of surface sediments, particulate organic matter, riverine sediments (RS), degraded vegetation (DV), and living vegetation (LV) indicating the corresponding position or source in the fjord system. RS is the average value for sediments <125 μm from the rivers Aldunate, Ventisquero, Cisnes, Cuervo, and Condor; DV is the average value of woody debris from leaves and wood fragments recovered from rivers; LV is the average value of nine species of living vegetation. $C_{24–32}$ FA concentrations were normalized by

organic carbon (mg FA g C_{org}^{-1}). $C_{24–32}$ ACL is the average chain length index = ($\Sigma[C_i]$ x i)/$\Sigma[C_i]$, for i = 24–32 where C_i = concentration *n*–alkanoic acid containing i carbon atoms. CPI is the Carbon Preference Index = sum of even $C_{24–32}$/sum of odd $C_{23–31}$. Gray circles for N/C, $\delta^{13}C$, and $\delta^{15}N$ represent particulate organic matter values.

Figure 4. Histograms of the distribution of homologues (percentage) of *n*–$C_{16–32}$ alkanoic fatty acid leaf waxes extracted from surface sediment (black bars), river sediment (white bars), degraded land vegetation (dashed bars), and living land vegetation (grey bars).

Figure 5. Relationship between geochemical data. (a) $\delta^{13}C$ and $\delta^{15}N$, (b) $\delta^{13}C$ and N/C, (c) $\delta^{15}N$ and N/C for surface sediments, particulate organic matter, and marine and terrestrial end–members. Marine end–members are represented by surface sediment at St. 1 (this study) and surface sediments from the continental slope taken from Hebbeln et al. (2000). Terrestrial end–members are represented by the average of the sedimentary fraction <125 µm from rivers and degraded and living vegetation. Data from farmed fish feces and pellet feed are from Sarà et al. (2004). Error bars represent the standard deviation whereas boxes display the range values of end–members. R^2 is the coefficient of determination from the linear fit (pellet feed and farmed fish feces data were not included in the equation).

Figure 6. Relative contributions of marine and terrestrial organic matter in surface sediments of the northern Patagonia fjord system. Values were derived from the mixing equation based on $\delta^{13}C$ values of marine and terrestrial end–members. Surface salinity (1 m water depth) was obtained from Silva et al. (1997).

Tables

Table 1. Location of sampling stations and data from the literature used in this work.

Sample	Station	Location	Latitude	Longitude	Depth (m)
Marine sediment	1	Off Boca del Guafo	43°45'10"S	74°37'29"W	240
	6	Moraleda Channel	43°59'26"S	73°21'95"W	176
	33	Jacaf Fjord	44°20'01"S	72°58'17"W	582
	42	Puyuhuapi Fjord	44°55'21"S	73°18'44"W	320
	40	Puyuhuapi Fjord	44°49'48"S	72°56'07"W	260
	39	Puyuhuapi Fjord	44°43'64"S	72°42'87"W	160
	36	Puyuhuapi Fjord	44°26'21"S	72°36'66"W	219
	35	Ventisquero Sound	44°21'37"S	72°34'95"W	52
	29	Quitralco Fjord	45°46'87"S	73°30'52"W	114
	29A	Quitralco Fjord	45°45'36"S	73°28'04"W	112
	30A	Quitralco Fjord	45°40'86"S	73°23'39"W	110
	30	Quitralco Fjord	45°40'19"S	73°17'11"W	269
	28	Cupquelan Fjord	46°08'65"S	73°29'73"W	239
	27	Elefantes Gulf	46°29'06"S	73°48'25"W	112
[a]Particulate organic matter	33	Jacaf Fjord	44°20'01"S	72°58'17"W	5
	42	Puyuhuapi Fjord	44°55'21"S	73°18'44"W	5
	40	Puyuhuapi Fjord	44°49'48"S	72°56'07"W	5
	36	Puyuhuapi Fjord	44°26'21"S	72°36'66"W	5
	35	Ventisquero Sound	44°21'37"S	72°34'95"W	5
	29A	Quitralco Fjord	45°45'36"S	73°28'04"W	5
	28	Cupquelan Fjord	46°08'65"S	73°29'73"W	5
	22A	Costa Channel	45°29'53"S	73°30'83"W	5
	17A	Aysén Fjord	45°17'30"S	73°10'15"W	5
Riverine sediment	Aldunate	Jacaf Fjord	44º18'S	72º51'W	–
	Ventisquero	Ventisquero Sound	44º22'6"S	72º35'W	–
	Cisnes	Aysén Fjord	44º44'5"S	72º43'W	–
	Cuervo	Aysén Fjord	45º21'S	73º03'5"W	–
	Condor	Aysén Fjord	45º28'S	72º54'5"W	–
Fresh vegetation	Cisnes River	Aysén Fjord	44º44'5"S	72º43'W	–
	Mulchey Island	Moraleda Channel	44º08'6"S	73º28'5"W	–
	Melchor Island	Moraleda Channel	45º03'S	73º43'W	–
[b]Open ocean sediment	GeoB 3312–2	Continental slope	41º00'5"S	74º20'20"W	583
	GeoB 3313–3	Continental slope	41º00'0"S	74º27'00"W	851
	GeoB 3314–2	Continental slope	41º36'2"S	74º58'80"W	1652
	GeoB 3316–1	Continental slope	41º56'2"S	75º12'80"W	2574
	GeoB 3317–6	Continental slope	42º00'8"S	75º18'10"W	2923
	GeoB 3318–2	Continental slope	42º02'3"S	75º19'30"W	3207
	GeoB 3323–4	Continental slope	43º13'1"S	75º57'00"W	3697

[a]Particulate organic matter collected from the ship's inlet (5 m water depth)

[b]Obtained from Hebbeln et al. (2000)

Table 2. Geochemistry of coastal surface sediments, riverine sediments, degraded and living vegetation, and end–member values of the northern Patagonia fjord system.

Sample & Station	C_{org}[a] (wt%)	TN[b] (wt%)	C/N–ratio[c] (molar)	N/C–ratio[d] (molar)	$\delta^{13}C_{org}$[e] (PDB ‰)	$\delta^{15}N$[f] (‰)	*n*–acids[g] (µg gdw^{-1})	*n*–acids[h] (mg gC_{org}^{-1})	ACL_{24-32}[i]	CPI[j]
Surface sediment										
1	1.0	0.1	9.6	0.104	–19.1	8.7	0.5	0.1	28.2	3.8
6	2.1	0.3	9.8	0.102	–20.2	8.3	4.9	0.2	27.8	3.9
33	3.4	0.4	10.5	0.095	–21.1	8.1	15.9	0.5	27.3	3.5
42	2.9	0.3	10.2	0.098	–20.9	9.0	n.d.	n.d.	n.d.	n.d.
40	2.3	0.2	14.7	0.068	–24.7	6.7	29.0	1.3	27.0	3.4
39	2.7	0.2	16.9	0.059	–28.0	1.4	29.0	1.1	26.7	3.0
36	1.3	0.1	14.3	0.070	–24.2	6.4	12.7	0.9	27.0	3.3
35	2.2	0.2	13.7	0.073	–24.7	6.4	17.4	0.8	27.2	3.3
29	0.5	0.1	10.1	0.099	–22.1	7.9	2.0	0.4	27.4	3.3
29A	1.4	0.1	12.2	0.082	–23.3	7.5	8.7	0.6	25.4	3.3
30A	2.1	0.2	11.6	0.087	–23.2	7.8	11.1	0.5	27.3	3.2
30	3.0	0.3	12.9	0.078	–23.6	8.0	14.6	0.5	27.3	3.1
28	0.8	0.1	14.3	0.070	–25.3	5.7	1.6	0.2	27.4	2.8
27	0.5	0.0	15.8	0.063	–24.9	6.0	8.4	1.6	27.0	4.2
Riverine sediment[k]										
Aldunate	1.2	0.1	16.0	0.062	–26.7	2.4	5.3	0.4	27.0	2.5
Ventisquero	0.2	0.0	16.4	0.061	–27.8	–1.1	1.8	0.8	27.4	3.3
Cisnes	0.4	0.0	15.1	0.066	–26.9	0.7	3.1	0.8	27.1	2.9
Cuervo	1.0	0.1	16.6	0.060	–27.2	1.2	2.4	0.3	27.0	2.8
Condor	5.7	0.4	16.1	0.062	–30.1	–1.0	11.0	0.2	26.8	2.9
Degraded vegetation[l]										
Ventisquero	20.8	0.5	45.5	0.022	–29.0	–3.7	3.5	0.0	26.2	6.1
Cisnes	27.6	0.7	45.3	0.022	–28.5	–2.0	2.6	0.0	26.8	9.3
Cuervo	15.1	0.5	32.7	0.031	–29.0	–2.1	0.9	0.0	26.0	6.6
Living vegetation[m]										
**Nothofagus* sp.	44.0	1.0	50.3	0.020	–32.0	–4.3	615.7	1.4	27.3	7.1
**Nothofagus nitida*	43.5	0.9	54.7	0.018	–32.0	–0.6	64.1	0.1	27.3	14.4
**Drimys winteri*	44.6	1.1	49.4	0.020	–29.1	–2.4	21.5	0.0	25.9	8.3
***Chusquea* sp.	40.9	2.8	17.1	0.058	–32.2	2.8	46.4	0.1	26.4	2.1
†*Libertia chilensis*	43.9	1.7	29.8	0.034	–32.2	3.2	281.9	0.6	29.0	6.7
†*Juncus* sp.	41.4	1.7	29.1	0.034	–28.0	2.6	88.6	0.2	29.4	3.1
†*Bromus* sp.	41.7	2.1	23.7	0.042	–32.2	4.2	67.8	0.2	27.7	8.6
†*Scirpus* sp.	39.8	1.2	38.8	0.026	–28.2	6.7	263.2	0.7	27.5	4.4
††*Blechnum chilensis*	40.9	2.0	23.7	0.042	–26.6	–2.5	5.3	0.0	25.4	1.6
Particulate organic matter[n]	(mg L^{-1})	(mg L^{-1})								
33	43.3	8.6	5.9	0.171	–22.6	10.2	–	–	–	–
42	92.0	12.2	8.8	0.113	–19.2	9.3	–	–	–	–
40	61.2	8.9	8.0	0.124	–19.8	8.8	–	–	–	–
36	34.6	5.1	7.9	0.127	–18.3	9.7	–	–	–	–
35	7.4	1.1	7.8	0.128	–22.7	11.5	–	–	–	–
29A	155.2	27.4	6.6	0.151	–21.6	8.4	–	–	–	–
28	15.3	2.0	9.1	0.110	–20.7	9.4	–	–	–	–
22A	15.1	2.3	7.5	0.133	–22.2	7.7	–	–	–	–
17A	43.1	4.5	11.2	0.089	–19.1	9.5	–	–	–	–
Open ocean sediment[o]	–	–	8.8 ± 0.2	0.130±0.003	–19.2 ± 0.11	9.3 ± 0.11	–	–	–	–
Marine end–member[p]	–	–	7.9 ± 0.7	0.127±0.010	–19.8 ± 0.3	9.9 ± 0.5	–	–	–	–
Terrestrial end–member[q]	–	–	30.6 ± 14.1	0.040±0.018	–29.3 ± 2.1	0.2 ± 3.0	–	–	–	–

[a] Organic carbon content
[b] Total nitrogen content
[c] Carbon/nitrogen molar ratio
[d] Nitrogen/carbon molar ratio. Recalculated as $(C/N)^{-1}$ from Hebbeln et al. (2000)
[e] Stable isotope composition of organic carbon
[f] Stable isotope composition of nitrogen

[g] Concentration of $C_{24–32}$ *n*–alkanoic fatty acids per gram of sediment
[h] Concentration of $C_{24–32}$ *n*–alkanoic fatty acids normalized by organic carbon
[i] Average chain length = $(\Sigma[C_i] \times i)/\Sigma[C_i]$, for i = 24–32 where C_i = concentration *n*–alkanoic acid containing i carbon atoms
[j] Carbon Preference Index = sum of even C_{24} to C_{32}/sum of odd C_{23} to C_{31}
[k] Sedimentary fraction from rivers <125 µm
[l] Vegetation debris isolated from riverine sedimentary fraction >355µm
[m] Living vegetation, where: *tree, ** understory, [†]shrubbery, and [††]fern
[n] Particulate organic matter collected from the ship's inlet (5 m)
[o] Averaged data from surface sediments from the continental slope off Chile between 41° S and 43°13'S and between 580 and 3700 m depth (see Table 1 in Hebbeln et al., 2000)
[p] Average value from Station 1 (this study) and Hebbeln et al. (2000)
[q] Average value between riverine sediments (<125 µm) and degraded and fresh vegetation
n.d. = not determined

Table 3. Comparison of the geochemistry of surface sediments from northern Patagonia with several estuarine and fjord systems in the world.

Location	C_{org}[a] %	TN[b] %	N/C[c]	$\delta^{13}C_{org}$[d] ‰	$\delta^{15}N$[e] ‰	Reference
Nordåsvannet Fjord, Norway	12.44	0.98	0.068	–23.9		Müller (2001)
Inner fjords of Spitsbergen, Svalbard	0.97–2.68	0.04–0.29	0.024–0.127	–25.2 to –21.9		Winkelmann and Knies (2005)
Continental shelf off Spitsbergen, Svalbard	0.53–2.41	0.04–0.25	0.056–0.147	–25.2 to –21.2		Winkelmann and Knies (2005)
Gulf of Gdansk, Baltic Sea, Poland			0.055–0.153	–22.0	0.0–12.0	Maksymowska et al. (2000)
Tay Estuary, Scotland	0.50–5.30	0.04–0.59	0.063–0.111	–26.6 to –23.2	2.6–10.6	Thornton and McManus (1994)
Labrador Sea, Canada	0.13–1.76	0.01–0.17	0.027–0.096	–22.6 to –21.2	6.6–8.4	Muzuka and Hillaire–Marcel (1999)
Laurentian Channel, Gulf of St. Lawrence, Canada	1.42–2.61	0.09–0.23	0.050–0.097	–22.4 to –21.7	5.8–8.9	Muzuka and Hillaire–Marcel (1999)
Continental shelf off Gulf of St. Lawrence, Canada	1.09–3.67	0.09–0.27	0.063–0.084	–22.1 to –21.3	7.5–8.4	Muzuka and Hillaire–Marcel (1999)
St. Lawrence Estuary and Saguenay Fjord, Canada	2.50–3.50	0.10–0.20	0.039–0.075			Louchouarn et al. (1997)
Upper St. Lawrence Estuary, Canada	0.53–2.92			–24.8 to –21.8		Louchouarn et al. (1997)
Chesapeake Bay, USA	0.17–5.04	0.02–0.57	0.042–0.231	–39.7 to –20.0	5.3–9.7	Zimmerman and Canuel (2001)
Chiloé and Aysén interior Seas, Chile	0.18–2.33	0.02–0.15	0.062–0.158	–26.2 to –20.4		Silva et al. (2009; this issue)
Northern Patagonia fjords	0.50–3.42	0.04–0.38	0.059–0.104	–28.2 to –19.1	1.3–9.0	This study
Central Patagonia fjords	0.25–2.14		0.090–0.158			Silva and Prego (2002); Aracena et al. (this issue)
Southern Patagonia fjords	0.98–10.32		0.074–0.129	–22.1 to –19.7		Silva and Prego (2002); Aracena et al. (this issue)

[a] Organic carbon content
[b] Total nitrogen content
[c] Nitrogen/carbon molar ratio. Recalculated from original references as $(C/N)^{-1}$
[d] Stable isotopic composition of organic carbon
[e] Stable isotopic composition of nitrogen

Table 4. Regional calculations of organic carbon accumulation and storage and CO_2 sequestration for the inner fjord system of northern Patagonia. Other fjords and estuarine systems in the Northern Hemisphere are included for comparison.

Location	Area[a]	porosity[b]	SR[c]	C_{org}[d]		$C_{org}AR$[e]		C_{org} BR[f]		C_{org-m}[g]	C_{org-m} BR[h]		C_{org-l} BR[i]		C_{org} burial[j]		C_{org-m} burial[k]		CO_2 seq[l]		CO_2 seq[m]	
	km^2		cm/yr	mg/gdw		$gC/m^2 * yr$		$gC/m^2 * yr$		%	$gC/m^2 * yr$		$gC/m^2 * yr$		ton/yr		tonC/yr		$ton/km^2 * yr$		ton/yr	
				min	max	min	max	min	max		min	max	min	max	min	max	min	max	min	max	min	max
Moraleda Channel	2,333	0.78	0.26	5.9	30.4	6.3	32.4	4.0	20.4	88.7	3.5	18.1	0.4	2.3	$9.2x10^3$	$4.8x10^4$	$8.2x10^3$	$4.2x10^4$				
Jacaf Fjord	236	0.77	0.28	28.0	34.2	33.4	40.8	21.0	25.7	86.3	18.1	22.2	2.9	3.5	$5.0x10^3$	$6.1x10^3$	$4.3x10^3$	$5.2x10^3$				
Ventisquero Sound	7.2	0.77	0.74	22.0	26.2	69.3	82.5	43.7	52.0	48.8	21.3	25.3	22.4	26.6	$3.1x10^2$	$3.7x10^2$	$1.5x10^2$	$1.8x10^2$				
Puyuhuapi Fjord	444	0.77	0.25	10.3	32.2	11.0	34.2	6.9	21.6	63.3	4.4	13.6	2.5	7.9	$3.1x10^3$	$9.6x10^3$	$1.9x10^3$	$6.1x10^3$				
Aysen Fjord	340	0.8	0.24	11.7	23.1	10.5	20.7	6.6	13.1	58.5	3.9	7.6	2.8	5.4	$2.3x10^3$	$4.4x10^3$	$1.3x10^3$	$2.6x10^3$				
Costa Channel	190	0.77	0.28	17.5	18.9	20.8	22.5	13.1	14.2	64.5	8.5	9.1	4.7	5.0	$2.5x10^3$	$2.7x10^3$	$1.6x10^3$	$1.7x10^3$				
Quitralco Fjord	116	0.79	0.47	5.1	30.3	4.6	55.3	2.9	34.8	66.1	1.9	23.0	1.0	11.8	$3.3x10^2$	$4.0x10^3$	$2.2x10^2$	$2.7x10^3$				
Cupquelan Fjord	125	0.64	0.14	2.2	9.0	1.9	8.4	1.2	5.3	42.0	0.5	2.2	0.7	3.1	$1.5x10^2$	$6.6x10^2$	$6.2x10^1$	$2.8x10^2$				
Elefantes Channel/San Rafael	490	0.77	0.25	0.6	7.4	0.7	7.9	0.4	5.0	49.5	0.2	2.5	0.2	2.5	$2.2x10^2$	$2.4x10^3$	$1.1x10^2$	$1.2x10^3$				
Total for study area	4281														$0.2x10^5$	$0.7x10^5$	$1.8x10^4$	$0.6x10^5$	15.3	53.1	$0.06x10^6$	$0.23x10^6$
Storfjord (Spitbergen)[n]	14,249							21.0	40.0						$3.0x10^5$	$5.7x10^5$	$8.0x10^4$	$2.5 x10^5$	19.7	63.2	$0.28x10^6$	$0.90x10^6$
Nordasvannet fjord, Norway[o]	4.6							2.2							$1.0x10^1$							
Saguenay fjord, Canada[p]	360							24.5	291.0						$8.8x10^3$	$1.0x10^5$						
Laurentian Channel, Canada[q]	25,000							2.0	4.0						$0.5x10^5$	$1.0x10^5$						
Gulf of St. Lawrence, Canada[r]	75,000							5.5	6.4						$4.1x10^5$	$4.8x10^5$						
Gulf of St. Lawrence, Canada[s]	75,000							0.8	2.5						$0.5x10^5$	$1.9x10^5$						

[a] Calculated using Google Earth
[b] Obtained from Silva et al. (1998a). Stations with a value of 0.77 correspond to an average value for the entire region
[c] Sedimentation rates from Rojas (2002), Salamanca and Jara (2003), Rojas and Silva (2005), Sepúlveda et al. (2005)
[d] Organic carbon content; from this study and from Silva et al. (1998a)
[e] Accumulation rate of organic carbon [C_{org} x SR x (porosity – 1) x bulk density]; calculated assuming a bulk density of 1.85 g/cm^3

[f] Burial rate of organic carbon assuming a maximum preservation efficiency for the entire study area of 63% (Sepúlveda et al., 2005)
[g] Fraction of marine–derived organic carbon. Obtained using the mixing equation based on local $\delta^{13}C$ end–members (see text for further details). Calculations for Moraleda Channel and Aysén Fjord were obtained using $\delta^{13}C$ data from Silva et al. (this issue) and Pinto and Bonert (2005)
[h] Burial rate of marine–derived organic carbon. Obtained using C_{org} BR and the percentage of $C_{org–m}$
[i] Burial rate of terrestrial–derived organic carbon. Obtained as the difference between C_{org} BR and $C_{org–m}$ BR
[j] Organic carbon burial per fjord and total
[k] Marine organic carbon burial per fjord and total
[l] CO_2 sequestration for the entire study area. Calculated using the stoichiometry of photosynthesis (see text)
[m] CO_2 sequestration per km^2
[n] Winkelmann and Knies (2005)
[o] Müller (2001)
[p] St–Onge and Hillaire–Marcel (2001)
[q] Louchouarn et al. (1997)
[r] Silverberg et al. (2000)
[s] Muzuka and Hillaire–Marcel (1999)

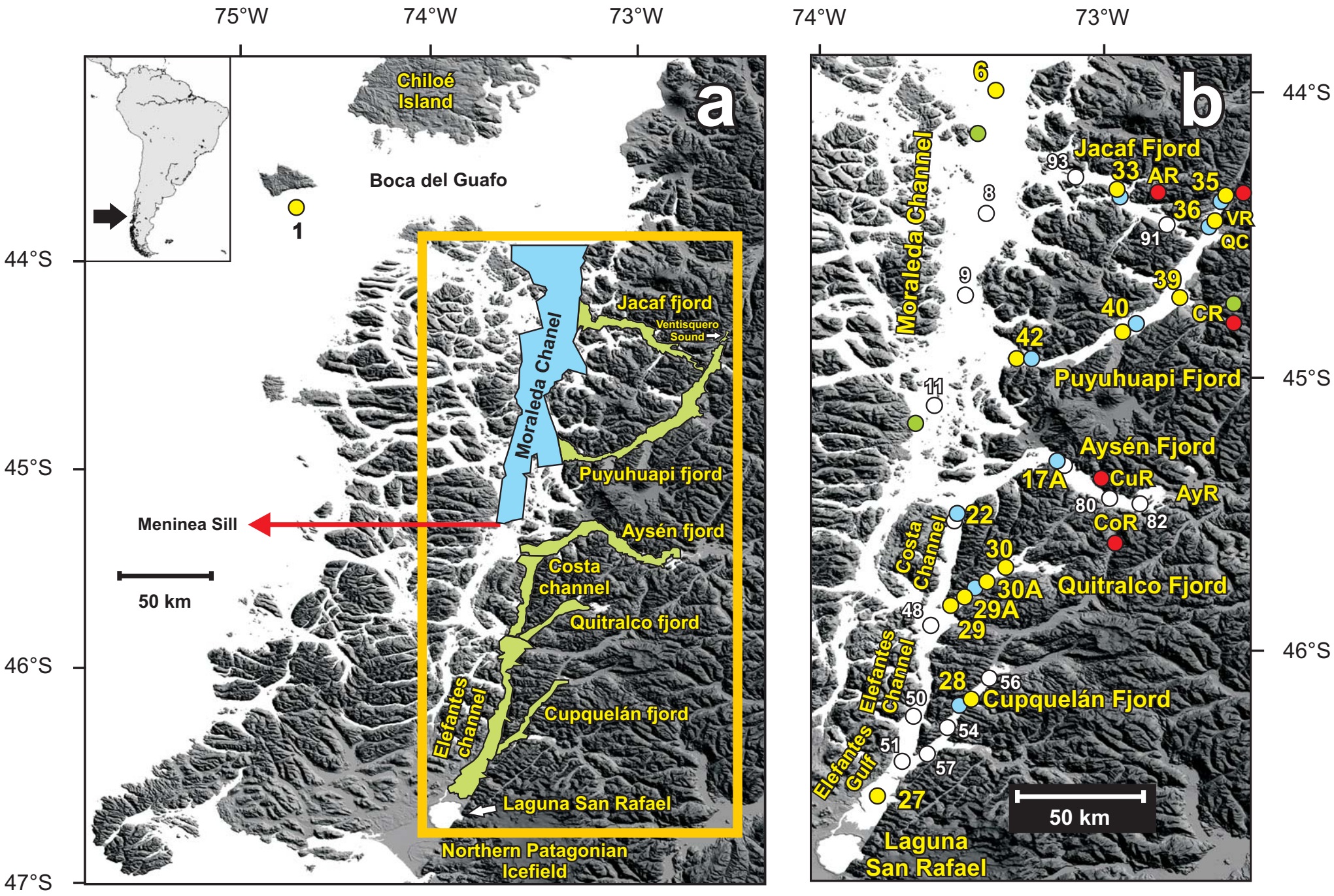
75°W
74°W
73°W
44°S
45°S
46°S
47°S
a
Chiloé Island
Boca del Guafo
1
Jacaf fjord
Ventisquero Sound
Moraleda Chanel
Puyuhuapi fjord
Aysén fjord
Costa channel
Quitralco fjord
Elefantes channel
Cupquelán fjord
Laguna San Rafael
Meninea Sill
50 km
Northern Patagonian Icefield
74°W
73°W
44°S
45°S
46°S
b
6
Moraleda Channel
8
9
11
93
Jacaf Fjord
33
AR
35
36
VR
QC
91
39
40
CR
42
Puyuhuapi Fjord
Aysén Fjord
17A
CuR
AyR
80
CoR
82
22
Costa Channel
30
30A
Quitralco Fjord
29A
48
29
Elefantes Channel
28
56
Cupquelán Fjord
50
54
51
57
Elefantes Gulf
27
50 km
Laguna San Rafael

FIGURE 1

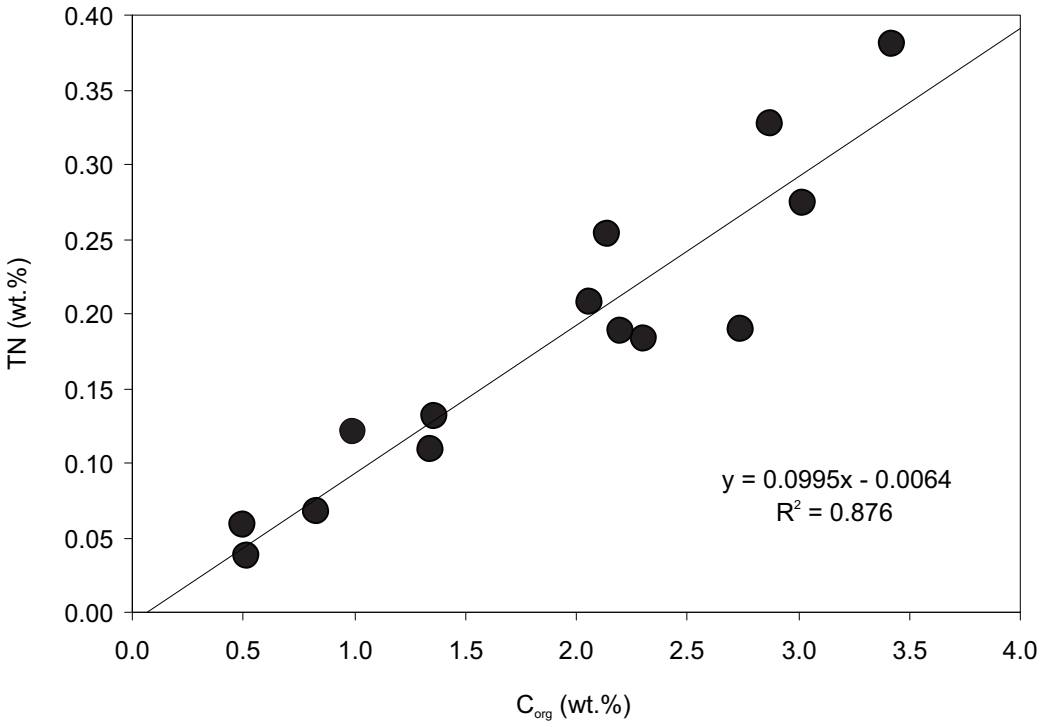
0.40
0.35
0.30
0.25
0.20
0.15
0.10
0.05
0.00
TN (wt.%)
0.0
0.5
1.0
1.5
2.0
2.5
3.0
3.5
4.0
C org (wt.%)
y = 0.0995x - 0.0064
R2 = 0.876

FIGURE 2

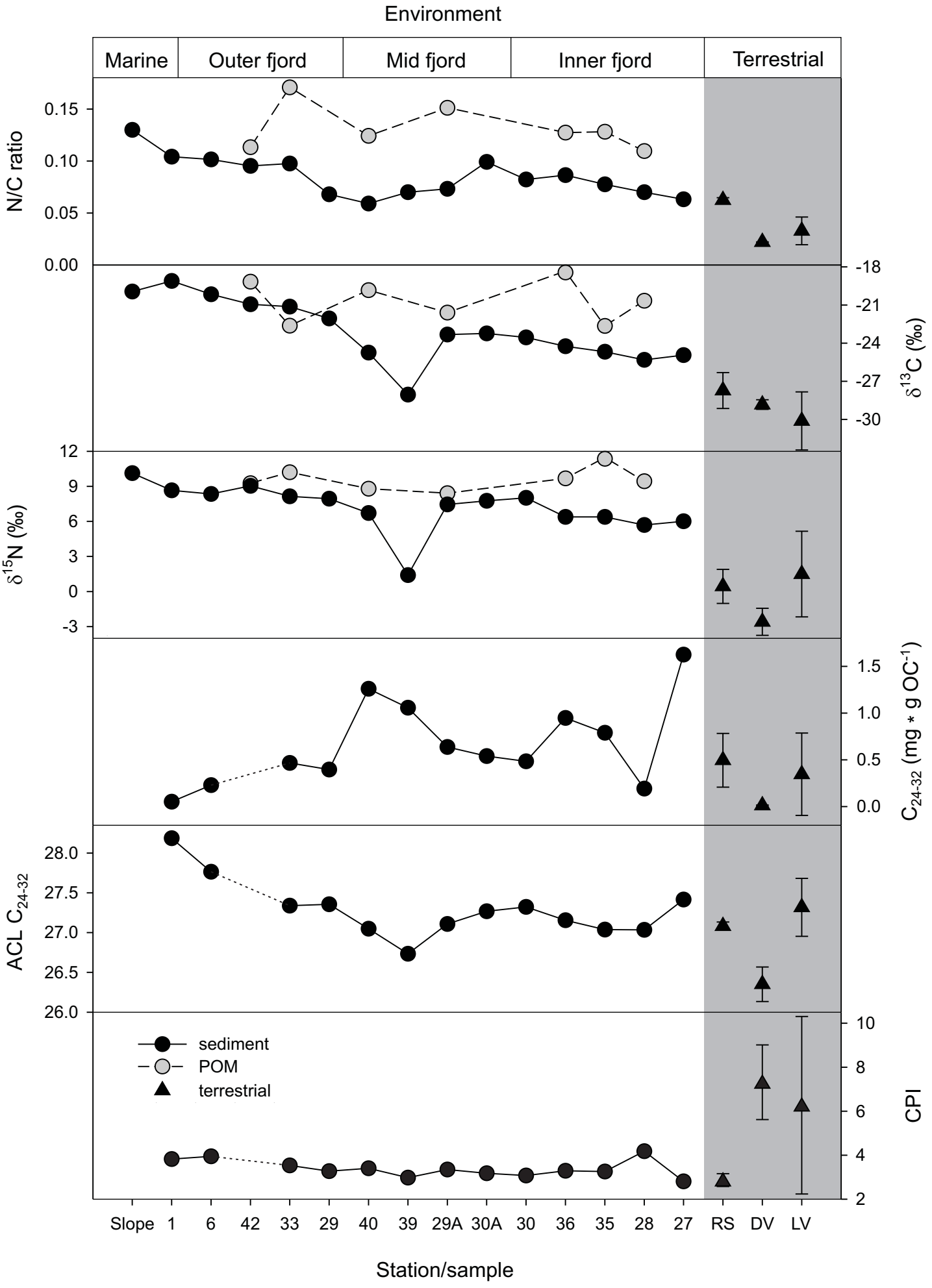
Environment
Marine
Outer fjord
Mid fjord
Inner fjord
Terrestrial
N/C ratio
0.15
0.10
0.05
0.00
δ13C (‰)
-18
-21
-24
-27
-30
δ15N (‰)
12
9
6
3
0
-3
C24-32 (mg * g OC-1)
1.5
1.0
0.5
0.0
ACL C24-32
28.0
27.5
27.0
26.5
26.0
CPI
10
8
6
4
2
sediment
POM
terrestrial
Slope
1
6
42
33
29
40
39
29A
30A
30
36
35
28
27
RS
DV
LV
Station/sample

FIGURE 3

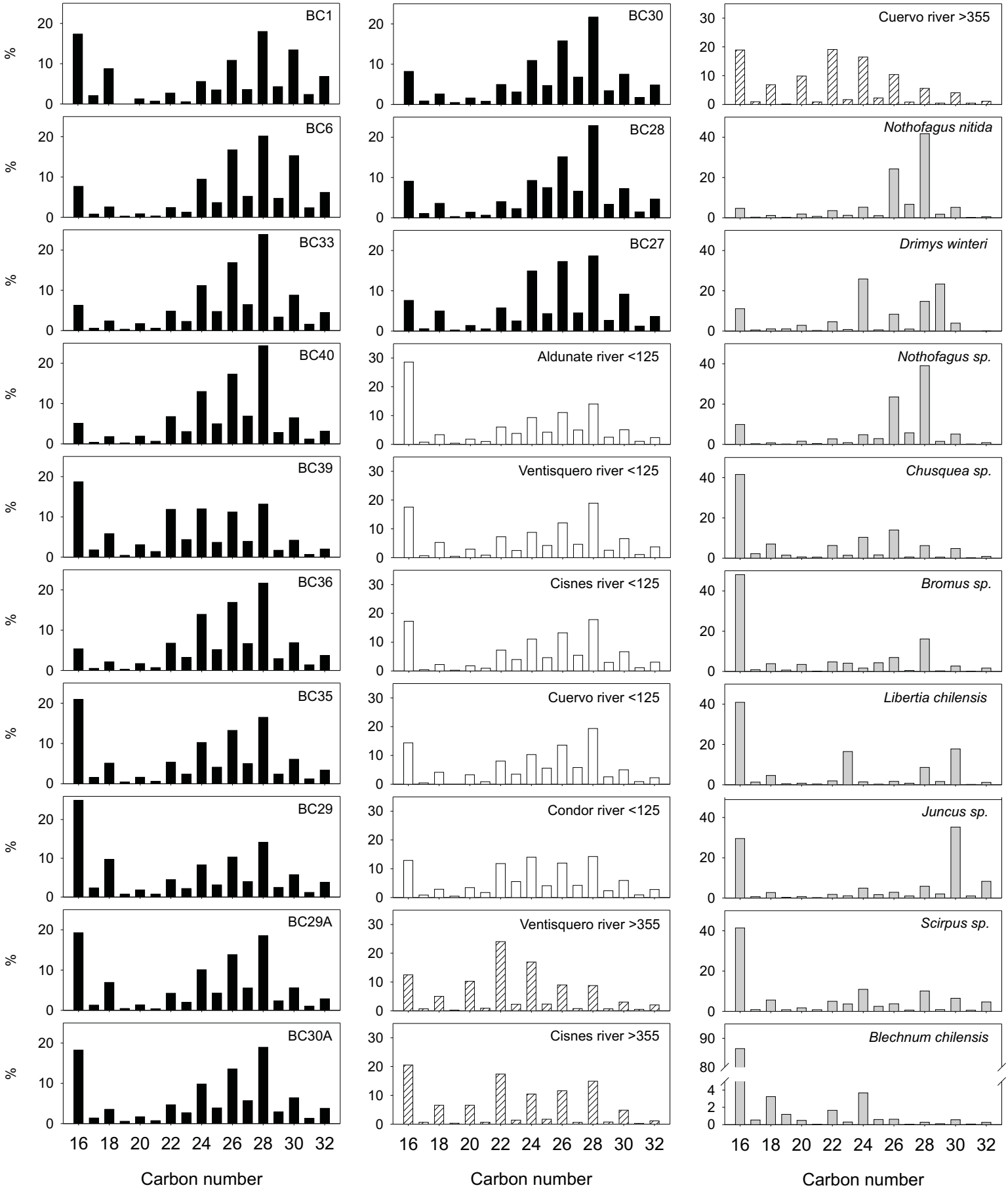
BC1
BC30
Cuervo river >355
BC6
BC28
Nothofagus nitida
BC33
BC27
Drimys winteri
BC40
Aldunate river <125
Nothofagus sp.
BC39
Ventisquero river <125
Chusquea sp.
BC36
Cisnes river <125
Bromus sp.
BC35
Cuervo river <125
Libertia chilensis
BC29
Condor river <125
Juncus sp.
BC29A
Ventisquero river >355
Scirpus sp.
BC30A
Cisnes river >355
Blechnum chilensis
%
16 18 20 22 24 26 28 30 32
Carbon number

FIGURE 4

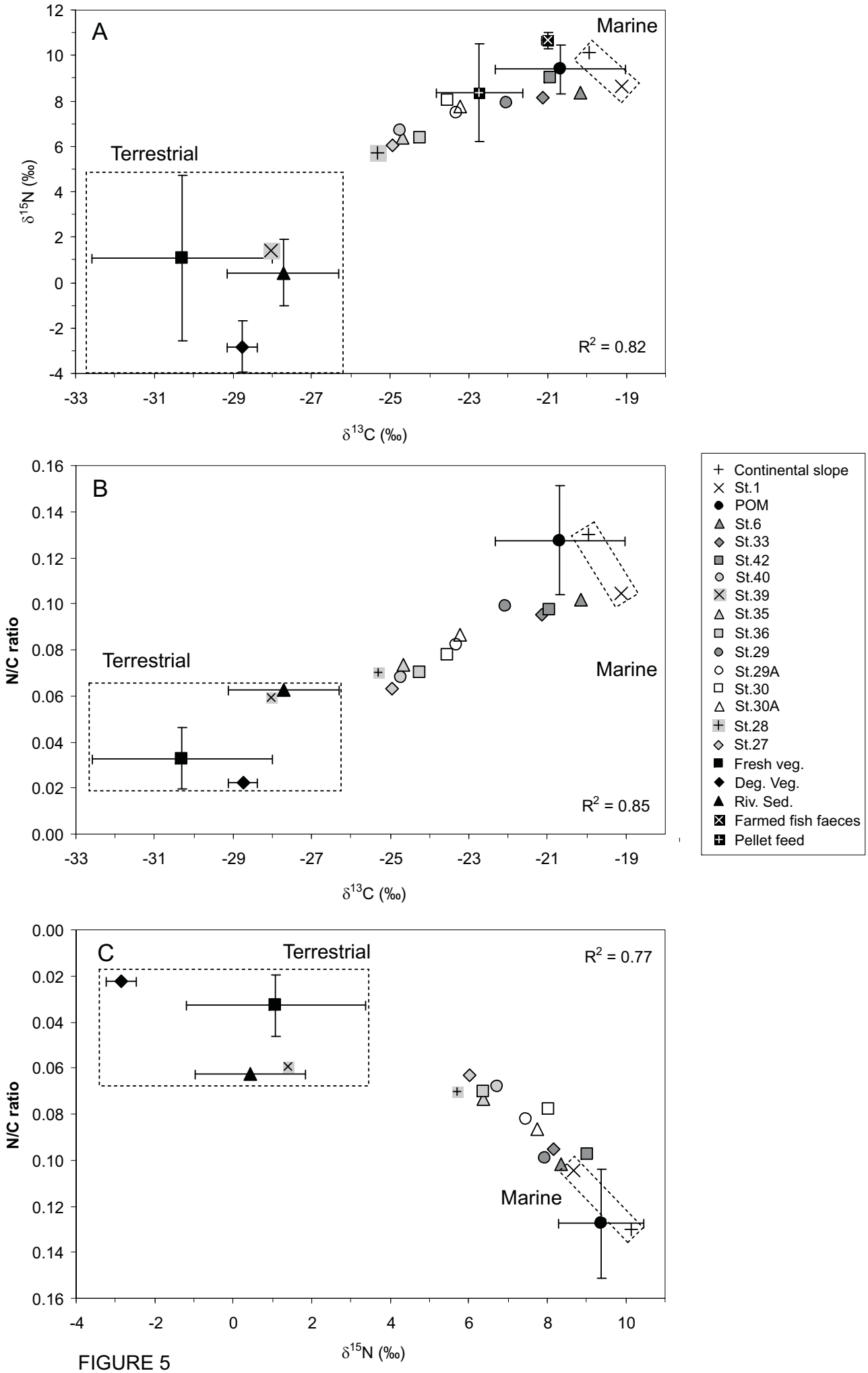
A
Marine
Terrestrial
R^2 = 0.82
δ^{15}N (‰)
δ^{13}C (‰)
B
Terrestrial
Marine
R^2 = 0.85
N/C ratio
δ^{13}C (‰)
C
Terrestrial
R^2 = 0.77
Marine
N/C ratio
δ^{15}N (‰)
Continental slope
St.1
POM
St.6
St.33
St.42
St.40
St.39
St.35
St.36
St.29
St.29A
St.30
St.30A
St.28
St.27
Fresh veg.
Deg. Veg.
Riv. Sed.
Farmed fish faeces
Pellet feed

FIGURE 5

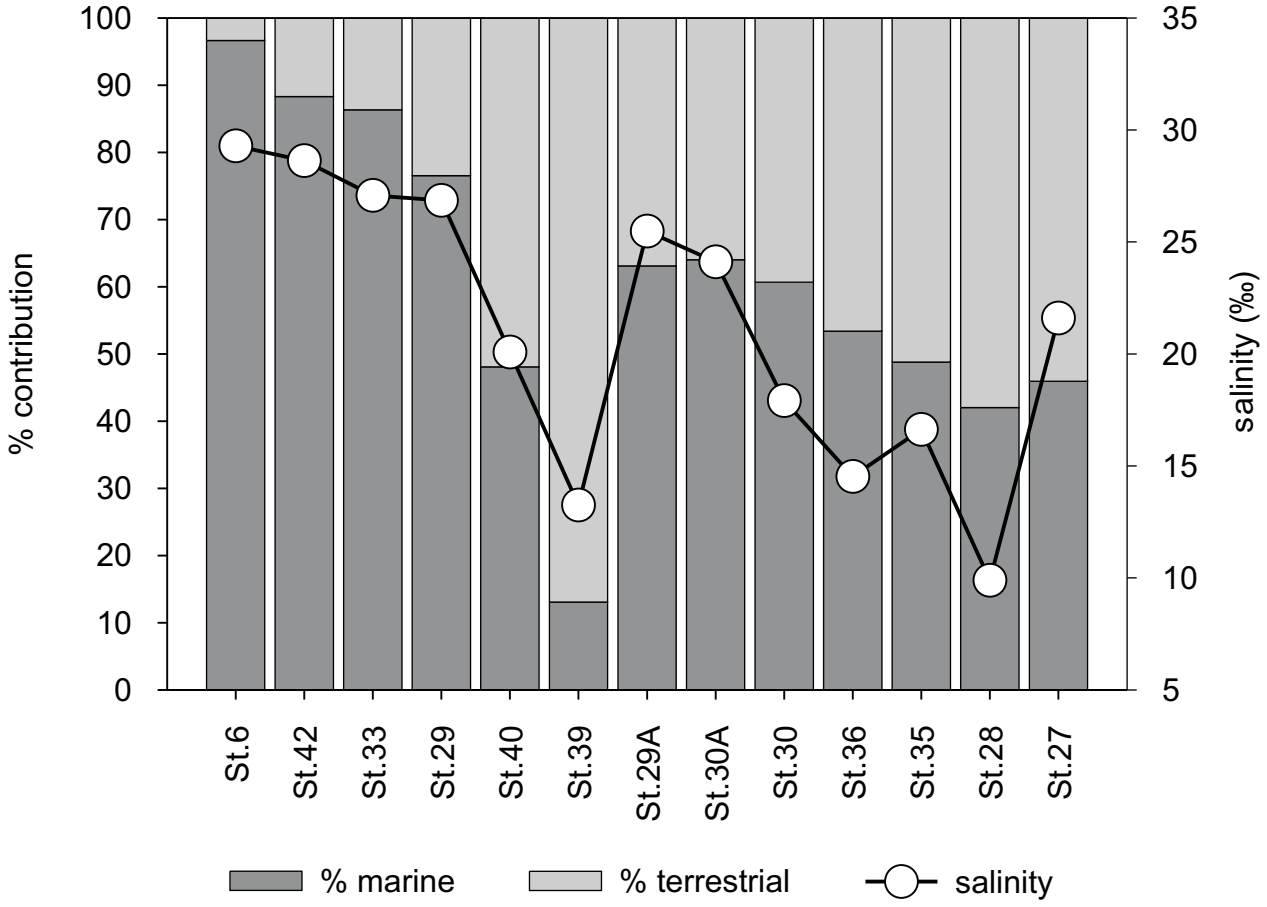
100
90
80
70
60
50
40
30
20
10
0
% contribution
35
30
25
20
15
10
5
salinity (‰)
St.6
St.42
St.33
St.29
St.40
St.39
St.29A
St.30A
St.30
St.36
St.35
St.28
St.27
% marine
% terrestrial
salinity

FIGURE 6